

## **A geometric approach to understand biological responses to environmental fluctuations from the perspective of marine organisms**

Gimenez Noya, Luis

### **Marine Ecology Progress Series**

DOI:  
[10.3354/meps14414](https://doi.org/10.3354/meps14414)

Published: 19/10/2023

Peer reviewed version

[Cyswllt i'r cyhoeddiad / Link to publication](#)

*Dyfyniad o'r fersiwn a gyhoeddwyd / Citation for published version (APA):*  
Gimenez Noya, L. (2023). A geometric approach to understand biological responses to environmental fluctuations from the perspective of marine organisms. *Marine Ecology Progress Series*, 721, 17-38. <https://doi.org/10.3354/meps14414>

#### **Hawliau Cyffredinol / General rights**

Copyright and moral rights for the publications made accessible in the public portal are retained by the authors and/or other copyright owners and it is a condition of accessing publications that users recognise and abide by the legal requirements associated with these rights.

- Users may download and print one copy of any publication from the public portal for the purpose of private study or research.
- You may not further distribute the material or use it for any profit-making activity or commercial gain
- You may freely distribute the URL identifying the publication in the public portal ?

#### **Take down policy**

If you believe that this document breaches copyright please contact us providing details, and we will remove access to the work immediately and investigate your claim.

**A geometric approach to understand biological responses to environmental fluctuations  
from the perspective of marine organisms**

Luis Giménez<sup>1,2,\*</sup>

1. School of Ocean Sciences, Bangor University, LL59 5AB , Anglesey UK

2. Alfred-Wegener-Institut, Helmholtz-Zentrum für Polar- und Meeresforschung,  
Biologische Anstalt Helgoland, 27498 Helgoland, Germany

\*Corresponding author: Luis Giménez: School of Ocean Sciences, Bangor University, LL59  
5AB , Anglesey UK

Running title: Responses of marine biological systems environmental fluctuations

## Abstract

A main concern in marine ecology is understanding the mechanisms driving responses of biological systems to environmental fluctuations. A major issue is that each biological system (e.g. organism, ecosystem) experiences fluctuations according to its own intrinsic characteristics. For instance, how an organism experiences a thermal fluctuation, i.e as a long marine heatwave or as a mild pulse, depends on its thermal tolerance and developmental time, which can vary as the fluctuation is experienced. Here, I explore a geometric approach, considering the biological perspective. Environmental fluctuations are represented as points in a “space of fluctuations”. The biological perspective is then defined as a coordinate frame within that space. Coordinates are given by components (e.g. amplitude and time scale) characterising each environmental fluctuation, which are then transformed into biological scales, using biological traits (tolerance and biological time). Using simulations of organisms growing under thermal fluctuations with different characteristics, I show how this approach: (1) Enables to integrate physiology and phenology to better interpret biological responses to fluctuating environments. (2) Improves understanding of the role of adaptive plasticity as a rescue effect. (3) Facilitates understanding the effects of thermal fluctuations on additional organismal traits (e.g. body mass). I also discuss wider applications in the context of species persistence, coexistence, biodiversity, and ecosystem function in scenarios of extreme fluctuations.

**Keywords:** acclimation, fluctuating environments, marine heatwaves, multiple stressors, phenology, phenotypic plasticity, thermal tolerance

## 1. INTRODUCTION

One of the biggest challenges in marine ecology is understanding mechanisms driving responses of biological systems to environmental fluctuations (Thompson et al. 2013, Kroeker et al. 2020, Gerhard et al. 2023). Environmental fluctuations occur at several time scales (Chave 2013) and extreme fluctuations have increased over the past decades. For instance, marine and atmospheric heatwaves of period ranging from days to months have become more frequent, more extreme, and less coherent in the past 30 years (Russo et al. 2015, Hobday et al. 2016, Benedetti-Cecchi 2021). Ecologists are aware that fluctuating environments can drive biological systems through mechanisms that differ from those present in constant environments (Levins 1968, Sæther, B.-E. & Engen 2015, Denny 2019, Bernhardt et al. 2020). However, our mechanistic understanding of responses to environmental fluctuations is limited because most experiments are using static designs, i.e. manipulating an environmental variable but keeping each treatment level constant over time. Results from experiments with static designs do not correctly predict responses to fluctuating conditions. For instance, adaptive plasticity evolves strictly in fluctuating environments (Scheiner 2016); at the organismal level, adaptive plasticity may be triggered by a fluctuation after some environmental threshold is surpassed, but not necessarily if the average condition of the fluctuation is experienced. Above a threshold, important (or irreversible) damage, may lead to carry-over effects (Minuti et al 2022). At the population and community level, responses to mean conditions differ to those from extremes (Lynch et al. 2014). At the community level, fluctuations drive historical/legacy effects associated to the time scale of recovery time between fluctuations (Williams et al. 2011, Dal Bello et al. 2017). Storage effects and relative non-linearity are mechanisms sustaining species coexistence that operate strictly in fluctuating environments (Chesson 2018). Hence, in many cases we cannot use the information provided by most static experiments even if they represent the average condition of the fluctuation.

We need experiments manipulating the components characterising the fluctuations. Fluctuation components may be defined as the amplitude, average, maximum, minimum, time scale, and timing of a fluctuation (Jentsch et al. 2007, Gunderson et al. 2016, Donelson et al. 2018, Giménez et al. 2022). In the case of noise, such components may be defined as the intensity and the dominating frequency (Vasseur & Yodzis 2004), which have ecological and evolutionary consequences (Romero-Mujalli et al. 2021). Experiments provide mechanistic understanding (Benedetti-Cecchi 2003, 2006, Koussoropolis et al. 2017, Gunderson et al. 2016, Boyd et al, 2018, Gerhard et al. 2023) and are needed as a part of a wider set of methodologies

(Dawson et al. 2011, Thompson et al. 2013, Koussoropolis et al. 2017). The experimental study of effects of fluctuations on biological systems brings both logistical and conceptual challenges (Thompson et al. 2013, Giménez et al. 2021, 2022). Logistical challenges associated with the number of replications, have been addressed through specific experimental designs (Boyd et al. 2018, Kreyling et al. 2018). Issues associated with teasing apart the role of different components characterising a fluctuation have also been addressed in the case of disturbance events, with intensive effort into separating the effect of mean and temporal variance of a fluctuation (Benedetti-Cecchi 2003, 2006, Bertocci et al. 2005, 2007, Maggi et al. 2012).

In recent years there has been an intensive effort to generate a general framework to incorporate fluctuations into studies of effects of climate change on organisms (Gunderson et al. 2016, Boyd et al. 2018, Gerhard et al. 2023). Within the framework, a major gap is the consideration of organismal perspective (Jackson et al. 2021), given by how biological systems experience a fluctuation in relation to their own biological traits. The importance of studying effects of environmental fluctuations on biological traits is obvious and has been widely recognised. We can therefore use current information on critical biological traits, to develop a mathematical foundation and provide metrics to quantify fluctuation components, from the organismal perspective. For instance, recent studies have quantified the time scales of thermal fluctuations using biological time as a trait (time to metamorphosis: Giménez et al. 2022; generation time: Munch et al 2023). Some important facts (Fig. 1) motivating this approach are: (1) Biological time scales, such as generation time (or time to reproduction) are central traits with direct impact on fitness (Stearns 1986, chap. 6, Angilleta 2009, chap. 6). (2) Adaptive responses, driving to evolutionary rescue (Chevin et al. 2010), can vary with time scales ranging from short term plasticity (hardening) through acclimation to trans-generational plasticity and genetic adaptation (Gerken et al. 2015, Donelson et al. 2018). (3) In ectotherms, within species, increased temperature results in (a) strong non-linear effect on biological time through changes in metabolic rates (Gillooly, et al. 2002, Rombough 2003, Giménez 2011), (b) increases in aging rate (Burraco et al. 2020, Cayuela et al. 2021), and (c) increases in the speed of behavioural responses (kinetic effects of temperature on behaviour: Abram et al. 2017). Because in ectotherms, the above changes are the result of increases in kinetic energy within cells and tissues, it is likely that changes in environmental temperature also affects the time scale of adaptive plastic responses. Studies of the effects of temperature on biological time have shown that: (1) Whether multiple-stressor responses are additive or interactive depends on whether time is measured in “clock” vs biological units (Giménez et al 2022); this also

extends to how sensitive organisms are to a given stressor. (2) Re-scaling the equations of population dynamics to biological time, lead to more robust predictions of dynamics of ectotherms in seasonal environments (Munch et al 2023).

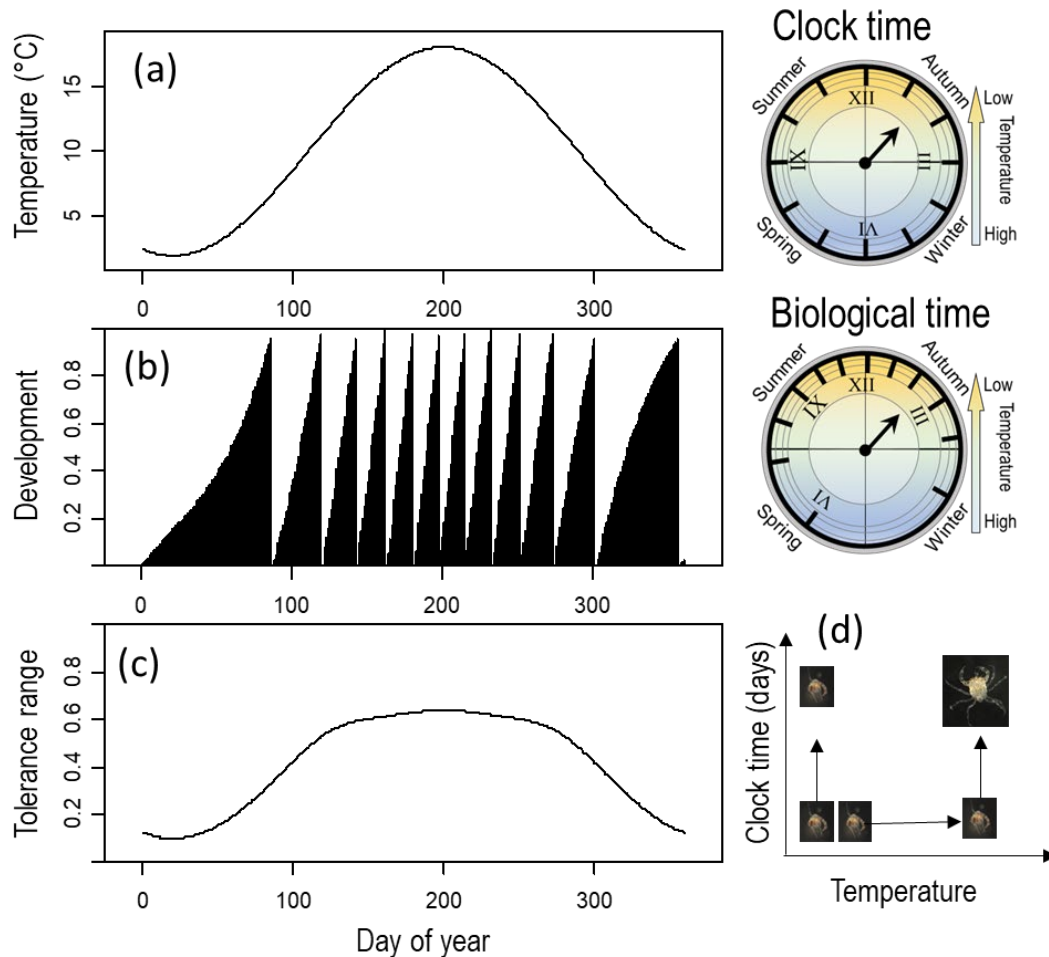


Figure 1. Simulated example of responses to thermal fluctuations in a marine ectotherm developing through 12 stages. (a) A seasonal thermal fluctuation and associated clock time where each of the clock 12 divisions represents a month and the colour gradient represents the temperature (for simplicity XII corresponds to the day of year of peak temperature). (b) Biological time: the cumulative proportion of development calculated as the proportion of development to each stage, using degree days (i.e. a stage is completed when the cumulative temperature reaches 280 °C days). Once a stage is reached, the cumulative proportion resets to zero and increases until a new stage is reached. In the associated biological clock, the position of the stages varies depending on temperature. Hence, the time marks in the biological and clock do not coincide. (c) Thermal fluctuation as experienced from the organism, calculated as the proportion of the upper thermal range (from the optimum to the upper thermal tolerance limit). The pattern of fluctuation is buffered with respect to the pattern in (a) because organisms acclimate to high temperature over the summer. (d) Illustration of an experiment where two sibling crab larvae are reared at different temperatures for a fixed amount of clock time, after which the sibling exposed to higher temperature is developmentally older than the one reared at low temperature. In (d) photographs by the author.

Because system experience must be multifactorial (i.e. depending on biological time plus other traits), we need a framework that consider additional traits as metrics of other fluctuation components. Hence, in this paper, I expand a previous framework, explored in Giménez et al. (2022), which did not consider a biological metric for the magnitude (e.g. intensity, amplitude, average) of an environmental fluctuation. A biological metric for fluctuation magnitude is critical for example to categorise a given fluctuation as an “extreme event”. This is relevant for instance in the context of the study of heatwaves, where definitions may be based on climatology or biology (Bailey & van de Pol 2015) and on different references or baselines against which fluctuations are compared (e.g. Hobday et al. 2016, Jacox 2019). We also need to account for intra and interspecific effects of environmental fluctuations and the associated mechanisms. Within species, tolerance is shaped by both adaptive (i.e. adaptive plasticity and genetic evolution: Donelson et al. 2018) and non-adaptive responses (e.g. carry-over effects and “silver spoon” maternal effects: Pechenik 2006, Uller et al. 2013, Ruiz-Herrera 2017). Mechanisms underpinning tolerance also occur at other levels of organization: populations may differ in their gene frequencies which drive portfolio effects (Schindler et al. 2015, Šargač et al. 2022) and communities differ in the species composition driving species complementarity (Cadotte et al. 2013), all acting as compensatory mechanisms. In those situations, tolerance should vary over time as a fluctuation is experienced. In synthesis, organismal experience (or that existing at other levels of organization) can be quantified as tolerance and biological time and is characterised by complex dynamics, which shape other biological responses.

The approach proposed here (thereafter called “space of fluctuations approach”, abbreviated as “SOFiA”), incorporates the perspective of the biological system in understanding biological responses to fluctuations. This is based on the idea (borrowed from differential geometry and physics: see e.g. Needham 2021) that there is no “absolute” perspective to characterise a fluctuation and its components; instead, there are different perspectives, from different systems (e.g. the human observer and an organism experiencing the fluctuation). This paper is structured as follows: First, I present SOFiA in a wider context aimed at making predictions of responses, given field-observed environmental fluctuations. Second, I present the core ideas (space of fluctuations and coordinate frames to quantify the organismal perspective). Third, I explore SOFiA using three cases at the organismal level. Fourth, I use a worked example of a simulated factorial experiment, manipulating fluctuation components to clarify the design and data needed to quantify the organismal perspective. My emphasis is on effects of thermal

fluctuations at the organismal level, but wider applications, on populations and ecosystems, are presented in the Discussion.

## 2. METHOD CONTEXT

The approach proposed here must be viewed as integrated into a wider framework (Fig. 2) combining field observations, experiments, and models predicting responses of biological systems to multiple fluctuating environmental drivers (Denny et al. 2009, Dawson et al. 2011, Koussoroplis et al. 2017, Gerhard et al. 2023). Thermal fluctuations (e.g. a heatwave) are characterised by a set of components, e.g. time scale, amplitude, cumulative intensity, rates of increase and decrease in temperature (see e.g. Hobday et al. 2016 for marine heatwaves). Field observations provide information on the range of fluctuation types (characterised by their components) that are then used to define the range of values considered in an experiment. The effects of thermal fluctuations are quantified using factorial-orthogonal experiments, teasing apart the effect of each component. The output of the experiment can then be used for predictions in the field or for parameterization of models (Fig. 2). Predictions in the field may be based, for instance, on scale transition theory, a method providing estimations of average responses from mean, variances and covariances of environmental variables (see worked example, Chesson 2012, Denny & Benedetti-Cecchi 2012, Dowd et al. 2015, Koussoroplis et al. 2017).

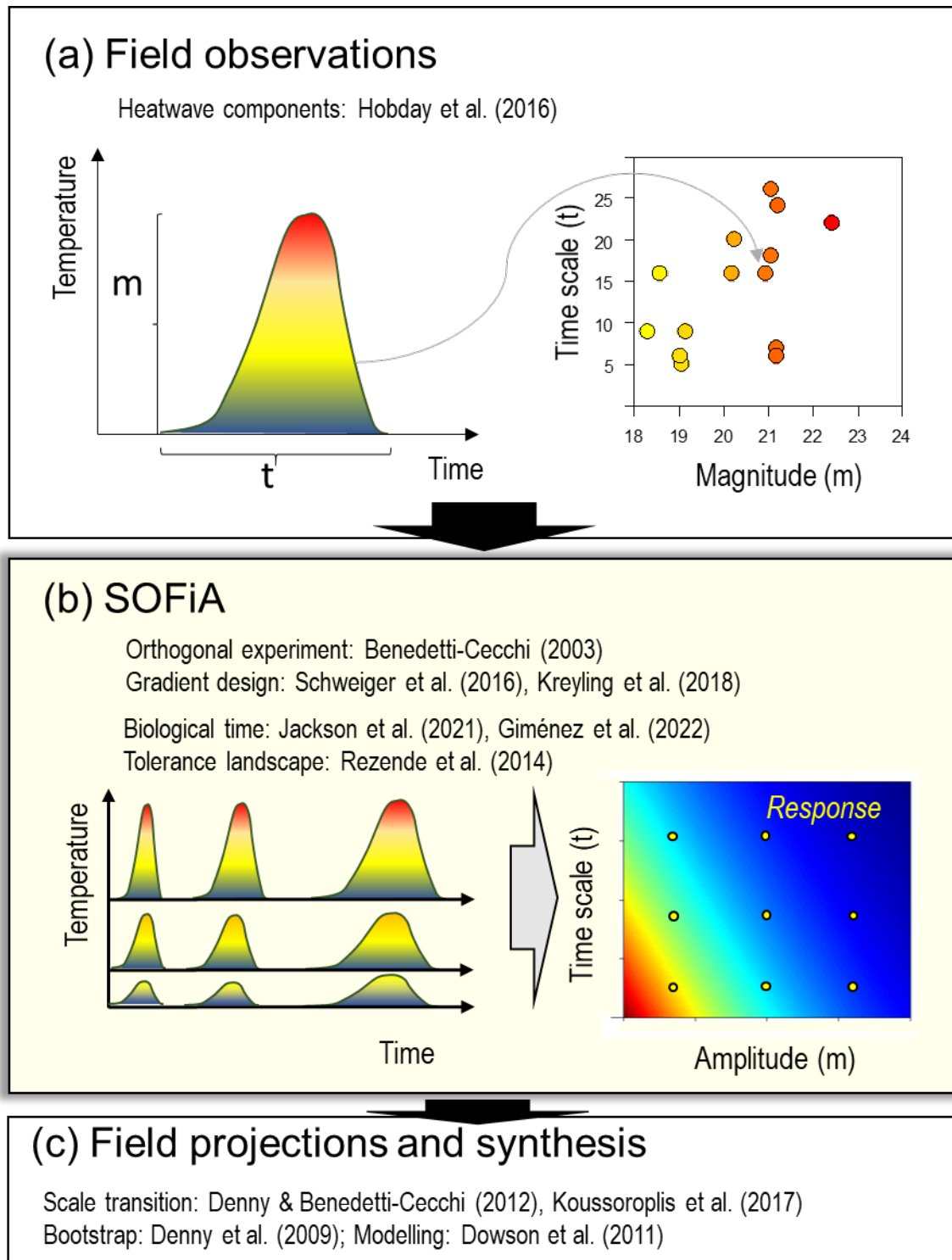
### 2.1 Experimental designs

The central point in SOFiA concerns the experimental phase: Orthogonal experiments are necessary to derive quantitative relationships between predictors and responses and are essential for the development of mechanistic models (Benedetti-Cecchi 2003). This argument is valid also when different environmental variables (or fluctuation components) co-vary in the field. In such a case, the experiment will provide information that is relevant to current environmental context, enable predictions of future scenarios where the covariation is broken (Benedetti-Cecchi 2003, Boyd et al. 2018) and cover for responses to rare events (Kreyling et al. 2014) such as extreme heatwaves. One may envisage an orthogonal experiment, considering fluctuations components as “fixed” predictors (then analysed with e.g. ANOVA) or as continuous predictors. The latter method is more appropriate for the approach presented here; it can be based on surface response designs (Box & Wilson 1951, Cottingham et al. 2005, Thompson et al. 2013, Kreyling et al. 2014, 2018, Schweiger et al. 2016).



Surface response designs will capture non-linear and non-additive responses to the fluctuation components present in the data. Because those responses are common in ecology and evolution (Levin 1998, Ruel & Ayres 1999, Schaffer 2009, Gunderson et al. 2016, Kroeker et al. 2020) surface response designs are better suited to improve ecological models than the ANOVA type design (except when the predictor in question is categorical). Surface response designs also provide the appropriate response function needed in scale transition theory, developed to incorporate interactive and non-linear responses to environmental fluctuations (Koussoroplis et al. 2017).

The main issue with surface response designs is the large number of experimental units needed to cover the predictor space defined by the fluctuation components. For example, consider an experiment with two components and a maximum of 90 replicate units; 10 replicate units per treatment combination would constraint the experiments to 9 locations (i.e. 3x3 combinations of component values) in the predictor space. A potential solution is to use sequential experiments covering different regions of the predictor space at each stage (Box & Wilson 1951); this may be problematic if replicates are likely to vary in time for some reason other than the experimental random variation. An alternative solution is to either optimise the number of replicates or to use un-replicated designs, a technique known as “gradient analysis” (Kreyling et al. 2018); for instance, at 90 replicate units, one may define 90 locations (as a 9x10 grid), allocating one unit each. Modelling exercises show that designs with low or no replication, but many locations, outperform replicated designs with fewer locations in detecting non-linear responses (Schweiger et al. 2016, Kreyling et al. 2018).



226

227 Figure 2. SOFiA in the wider context of scaling experiments to predictions under field  
 228 conditions. (a) Thermal fluctuations (e.g. heatwaves) vary considerably in amplitude ( $m$ ) and  
 229 time scale ( $t$ ). (b) In SOFiA, an orthogonal experiment is carried out simulating fluctuations of  
 230 different combinations of  $m$  and  $t$ ; a response (e.g., body size as a heat map, with values  
 231 decreased from red to blue) is quantified, at fixed locations (some represented as yellow  
 232 points). In addition, organismal traits are used as metric to define coordinate frames where the  
 233 additional biological responses are quantified. (c) Experimental results are used together with  
 234 field data for models, projections (i.e. scenario analysis) or predictions. The references cited  
 235 show the literature providing ideas concerning one or more steps.

## 2.2 Fluctuation components

We need an approach accounting for historical effects found at different levels of organization. For instance, at the organismal level, acclimation, and carry-over stress effects, are pervasive (Giménez 2006, 2020, Pechenik 2006, Marshall et al. 2016), and can drive recruitment in marine populations (Torres et al. 2016). Historical effects are also important at the community level and their evaluation requires the consideration of time scales explicitly in the design (e.g. see Dal Bello et al. 2017).

In the approach proposed here (Fig. 2b) fluctuations are characterised by an explicit time variable in addition to a magnitude variable (if only two components are considered). The use of the time variable enables to capture any historical effect in addition to rescale responses in biological time (see section of worked example, Giménez et al. 2022). The use of a time variable helps to move away from estimations of tolerance based keeping organisms at constant conditions or using ramp experiments that do not necessarily match the time scale of natural environmental fluctuations (Terblanche et al. 2011, Rezende & Santos 2012, Gunderson et al. 2016). The choice of the magnitude variable depends on the situation; I focus on the amplitude, to account for cases where historical responses are associated to threshold phenomena (e.g. acclimation being triggered after some temperature level is experienced). In the field, time scales and amplitudes of fluctuations can be estimated through direct observations or from statistical models such as Fourier analysis or polynomial fitting. In this set up, projections or predictions (see worked example) would be based on a response function matching the time scale of field-observed fluctuations.

## 3. THE SPACE OF FLUCTUATIONS

### 3.1 Coordinate frames

The central concept of SOFiA is that environmental fluctuations are characterised by a set of components and represented as points in a space. This multidimensional space resembles the one defined in multivariate analysis such as principal component analysis (or any other extension), where the principal components constitute a coordinate frame (Legendre & Legendre 1998). The space of fluctuations has also similarities with the concept space state disturbance representation (Turner et al. 1993, Fraterrigo & Rusak 2008) but mostly with the tolerance landscape (Rezende et al. 2014), defined by the intensity and duration of a thermal

stress. This concept may be expanded to a higher number of environmental variables (i.e. not only temperature), with the concomitant increase in the number of dimensions.

The second important point is that the metrics used to characterise thermal fluctuation components (e.g. for a heatwave: intensity measured in °C and time in days) is not unique nor absolute. Instead, each point in the space of fluctuations can be located using different coordinate frames. I define the “extrinsic frame” as the one defined by the “observer”, e.g. in clock time and °C. I also define the “intrinsic frame”, as representing how the biological system under study experiences the fluctuations, according to its own traits. For that purpose, I classify biological variables in three types: Type-1: Variables with units of magnitude (e.g. thermal tolerance range) or time (e.g. days to maturation) or driving tolerance and biological time; they give rise to the intrinsic frame. Type-2: Invariant responses: a biological response that occurs within the tolerance range, does not drive tolerance nor biological time and does not have units of time or magnitude. Type-3: Biological rates or sensitivities, i.e. those expressed as per unit of time or tolerance. The role of each variable will be introduced below.

As example, I focus on a study of the effect of thermal fluctuations on the body size (the invariant response) of a marine organism (e.g., invertebrate, fish), growing eventually to maturation. For the sake of the example, I assume that body size (the invariant response) does not drive tolerance or biological time. Biological time is the time to maturation; tolerance may be defined in a wide sense, i.e. as the range of preferred temperatures (Gvozdk 2018), based on the aerobic scope (Pörtner 2002), or a range defined from survival or knock-down temperatures (Tang et al. 2000). The same concepts can be applied to other levels of organization: for example, biological time can be quantified for populations (generation time), communities (time scale of change in richness: Ontiveros et al. 2021), and ecosystems (inverse of ratio of production/biomass). Tolerance can also be defined for populations (Gvozdk 2018) and communities (Vinebrooke et al. 2014).

In the extrinsic frame (Fig 2), the amplitude ( $= m$ ) is measured in °C and the time scale ( $= t$ ) in clock time, in e.g. days (see Supplement, Section 1, Table S1 for variables and constants). The biological time scale of a fluctuation ( $= \tau$ ) is a unitless quantity, corresponding to the proportion of time from birth to a relevant life history event (e.g., from birth to maturation). The biologically scaled amplitude of the fluctuation ( $= \mu$ ) is defined as a proportion of the thermal tolerance range of the organism, i.e., the capacity of the organism to withstand environmental fluctuations.

299 The next element of the space of fluctuations is the time at which observations are made. In the  
 300 idealised experiment (Fig. 3a), organisms (originated in the same population) are exposed to  
 301 fluctuations of different amplitude and time scales. All organisms are kept at the same initial  
 302 temperature, exposed to the fluctuations, and then returned to the initial temperature before a  
 303 measurement of body size is taken. The time at which body size is measured is expressed in  
 304 clock ( $t^*$ ) and biological scales ( $\tau^*$ ). The observation times considered here (there may be  
 305 several) occur *after* the fluctuation is experienced (Fig. 3a), i.e.  $t^* > t$  and  $\tau^* > \tau$ . Observations  
 306 must be done as the fluctuation occurs (see section of worked example), but organisms must  
 307 experience the full fluctuation before one can causally relate the response to the fluctuation  
 308 time scale. The time course of the invariant response will occupy the full space of fluctuations,  
 309 defined by the three axes: amplitude, time scale and observation time (Fig. 3b). Because we  
 310 assume that temperature drives developmental rates, the time points of observation, at fixed  
 311 clock time, will not coincide with those at fixed biological times (e.g. at maturation). Therefore,  
 312 observations at fixed clock vs biological times will lie on different types of surfaces slicing the  
 313 3D space defined by the fluctuation components and the observation time. The invariant  
 314 response, observed at fixed clock time lies on flat 2D time slices (Fig. 3b) of the space of  
 315 fluctuations. By contrast, the response observed at a fixed biological time (e.g. at maturation)  
 316 will lie on a curved surface (Fig. 3c), with its shape driven by the effect of temperature on the  
 317 developmental rate (see next paragraph). Consequently, the pattern shown by the biological  
 318 response will differ between the coordinate frames (Fig. 3c, d).

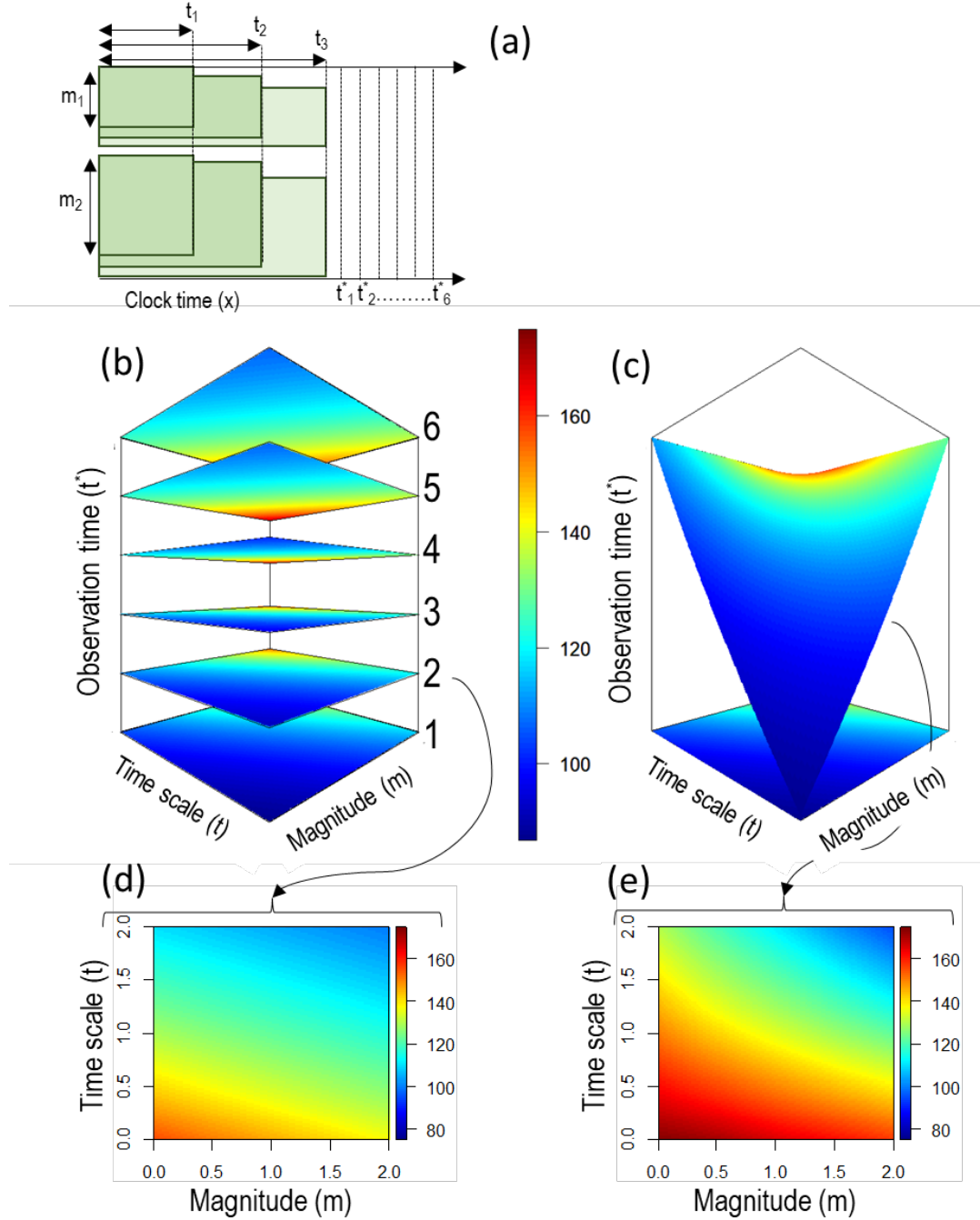


Figure 3. Idealised time course of an experiment quantifying the effect of thermal fluctuations on the body size (in arbitrary units) of an ectothermic organism at different times, including at size maturity, with the time of maturation driven by temperature. (a) Diagram of experimental design depicting a subset of the studied thermal fluctuations as rectangles of different magnitudes ( $m_1$ ,  $m_2$ ) and time scale ( $t_1$ ,  $t_2$ ,  $t_3$ ); clock observation time are given as  $t_1^*$ , ...,  $t_6^*$ . (b) At fixed clock time, body size varied through time, occupying the volume defined by  $m$ ,  $t$  and  $t^*$ . Body size, in response to  $m$  and  $t$ , lies on flat 2D slices (heat map) if observed at fixed clock times. (c) Body size at maturity however, lies on a curved surface defined by the effect of temperature on biological time. Panels (d) and (e) illustrate how such an idealised experiment would show that the effect of thermal fluctuations on body size would depend on the time coordinate  $t^*$  or  $\tau^*$ .

The next step is to define mathematical functions relating the components of the extrinsic frame ( $m$ ,  $t$  and  $t^*$ ) with those of the intrinsic one ( $\mu$ ,  $\tau$ , and  $\tau^*$ ). The functions linking clock with the biological time scales are given:  $\tau(t,m) = t \cdot L$  and  $\tau^*(t^*,m) = t^* \cdot L$  where  $L(t,m)$  is the developmental rate, i.e. the inverse of the clock time ( $=D$ ) required to reach a particular biological event (e.g. days to maturation). Importantly,  $L(t,m)$  is a function of the environmental fluctuation, not of the observation time (in line with above defined assumptions) and will be the inverse of the pattern shown by developmental time (Fig. 4a).

The biological scaled amplitude of the fluctuation,  $\mu(t,m)$ , is defined from thermal tolerance as  $\mu = mS$ . The function  $\mu$  (unitless) varies between 0 and any positive value and quantifies the magnitude of the environmental fluctuation relative to the organismal tolerance range. The function  $S$  is the inverse of the tolerance range ( $=E$ , Fig. 1d) which represents how sensitive is the biological system to the magnitude of the fluctuation. The case  $\mu = 1$  corresponds to a fluctuation that encompasses the full tolerance range, while  $\mu \rightarrow 0$  corresponds to situations where the organism is extremely eurytopic with respect to  $m$  ( $S \rightarrow 0$  when  $m$  is very small with respect to the tolerance range). I define  $E$  with respect to some threshold, for instance the so-called “knock out temperature” ( $= M_{out}$ , i.e., the temperature at which the organism dies or cease any activity, or it does not respond to stimuli). In synthesis,  $E$  is the mathematical expression of the capacity of the organism to tolerate a fluctuation.

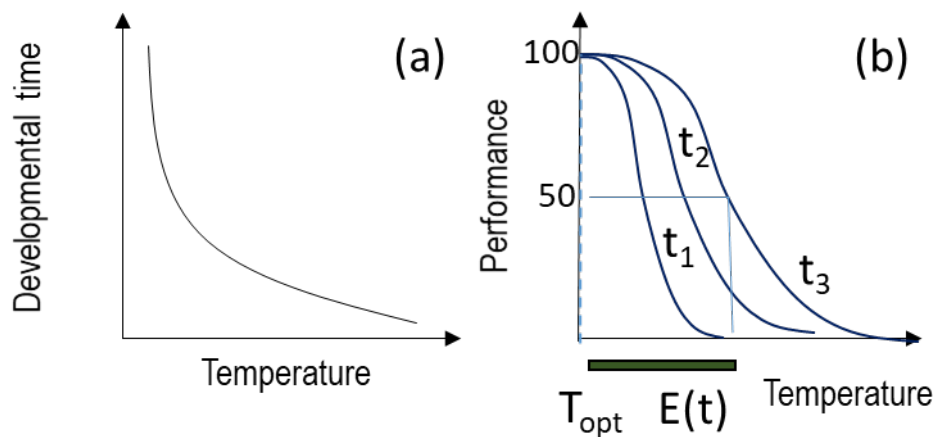


Figure 4. (a) The curve of developmental time, showing an non-linear decrease with temperature; this curve is modelled subsequently in Eqs. (4) & (5) in Results. Developmental time depends only on the amplitude of the thermal fluctuation  $D = D(m)$  as in the case of phenology models based on degree days, but such assumption does not restrict the analysis. (b) The tolerance range is defined for different fluctuations time scales ( $t_1, t_2, t_3$ ), used to obtain the term  $S$ , included subsequently in Eqs. (3) & (6) in Results.

## 3.2 Invariant responses

The invariant biological response (body size, Fig. 3b) is a type of response that does not drive tolerance and it is not a rate of change with respect to any of the coordinate frames. The invariant response exists within the limits stated by the biological time and tolerance, i.e. there is a “region of existence”, within the space of fluctuations. This response is represented by a continuous and differentiable function and the invariance property results in that:

$$R(t, t^*, m) = r(\tau, \tau^*, \mu) \quad (1)$$

The invariance property is the reason why rates are not considered at this stage. Rates are partial derivatives of the invariant response (see below) and their magnitude depend on the coordinate frame. The differentiability assumption enables to represent the effect of the thermal fluctuation on the response through partial derivatives with respect to the amplitude and period; the same idea applies to a general environmental fluctuation characterised by two or more quantitative descriptors. Hence, I define the effect of each variable of the invariant response as system of partial differential equations (PDE, Giménez et al. 2022), which in matrix formulation gives:

$$\begin{bmatrix} \frac{dR}{dm} \\ \frac{dR}{dt} \\ \frac{dR}{dt^*} \end{bmatrix} = \begin{bmatrix} \frac{d\mu}{dm} & \frac{d\tau}{dm} & \frac{d\tau^*}{dm} \\ \frac{d\mu}{dt} & \frac{d\tau}{dt} & \frac{d\tau^*}{dt} \\ \frac{d\mu}{dt^*} & \frac{d\tau}{dt^*} & \frac{d\tau^*}{dt^*} \end{bmatrix} \cdot \begin{bmatrix} \frac{dr}{d\mu} \\ \frac{dr}{d\tau} \\ \frac{dr}{d\tau^*} \end{bmatrix} \quad (2)$$

In a more compact notation, equation (2) may be written as  $\mathbf{R} = \mathbf{M}\mathbf{r}$  where  $\mathbf{R}$  and  $\mathbf{r}$  are vectors of derivatives of  $R$  and  $r$  respectively; both  $\mathbf{R}$  and  $\mathbf{r}$  contain biological rates and sensitivities with respect to magnitudes and time scales. The matrix  $\mathbf{M}$  transforms the rates of the intrinsic to the extrinsic frame; the inverse of  $\mathbf{M}$  will do the reverse transformation. In equation 2, the third entry of the second row of  $\mathbf{M}$  (in bold) is set to zero, when the observation time varies independently of the time scale of the fluctuation (fixed clock observation time). In practice,  $t^*$  is constrained to be longer than the longest fluctuation time scale used in an experiment; however, within such limits, one can observe the response at any desired time. In addition, the first two entries of the last row of  $\mathbf{M}$  (in bold) are set to zero because the observation time, ( $t^*$ ,  $\tau^*$ ) does not affect the biological tolerance ( $\mu$ ) nor the biological time scale of the fluctuation ( $\tau$ ). This follows from the fact that we ignore (for simplicity) the timing of the fluctuation as a component. In a more general case, such timing would be an additional component giving an extra dimension to the space of fluctuations.



Working with the response and the mapping functions is facilitated by two properties: (1) They should approximate to continuous and differentiable functions, so that the terms in  $\mathbf{M}$  and the derivatives of  $R$  exist. Modelling of tolerance is sometimes carried out through conditional functions but the alternative is to fit appropriate smooth functions to overcome the problem. (2) Mapping functions should be bijective (i.e. always increasing or decreasing), so as to provide a one-to-one, mapping. Such functions ensure the existence of direct and inverse maps, from each point of the extrinsic to each point of the intrinsic frame. Not all functions of developmental time are like this; instead, some show a minimum at an extreme high temperature threshold, followed by a maximum (Shi et al. 2016). Issues associated to (1) and (2) can be solved in practice by modelling different parts of the space of fluctuations as separate regions.

### 3.3 Scenarios of analysis

There are several scenarios for how the tolerance range and biological time drive the effect of the fluctuation on the invariant response. (1) The trivial scenario where neither  $E$  nor  $L$  are affected by the fluctuation traits. Both the extrinsic and intrinsic frames coincide and the effect of the fluctuation on the body mass does not change with the coordinate frame. (2) Where  $E$  is not affected by the fluctuation traits: in such a case (discussed in Giménez et al. 2022),  $\mu$  is proportional to  $m$ . (3) The scenario explored here, where both  $E$  and  $L$  depend on some property of the fluctuation being experienced.

The nature of the intrinsic frame depends on how biological time and tolerance are shaped by the fluctuations. I consider three cases: in Cases 1 and 2 increased temperatures would result in a deleterious effect on performance (Niehaus et al. 2012). Case 1 is based on simple functions that help to visualise and obtain qualitative understanding of the differences between the extrinsic and intrinsic frames. Case 1 is related to Case 2, which introduces empirical functions and enables a realistic view of chronic negative effects of fluctuations. Case 3 introduces adaptive plasticity by which the fluctuation has positive effects on the tolerance range. While in cases 1 and 2, I simulate the response observed at a fixed clock time, in case 3, I simulated the time course of the response.

## 4. RESULTS

The central point in SOFiA is that the space of fluctuations is represented using different coordinate frames, related through non-linear functions. It is important to clarify the two different types of representations: First, one can represent a time slice defined either at a fixed clock time or at a fixed biological time (see Fig. 3b, c). Second, for each time slice one can represent two projections, based respectively on the extrinsic (mt-projection) or intrinsic coordinates ( $\mu\tau$ -projection). For cases 1-3, I focus on time slices at fixed clock time (fixed  $t^*$ ): this represents the simplest possible experiment and enables better understanding of the different projections; the slice at a fixed biological time is explored in the worked example. Given a (fixed) time slice, fluctuations are plotted in the upper half of a plane (Fig. 5a, details in Supplement Section 2), where  $t > 0$  (fluctuations of negative time scale do not exist). In addition, none of the fluctuations will occur at  $m = 0$  or  $t = 0$  because such fluctuations do not exist either. For simplicity, I will assume that  $m > 0$  because experiments usually focus on either high or low temperature with respect to a thermal optimum, for which  $m$  can be conveniently rescaled to be positive. Hence, the fluctuations of interests are plotted in the first quadrant (Fig. 5a) and the properties mentioned below do no change if  $m$  is negative.

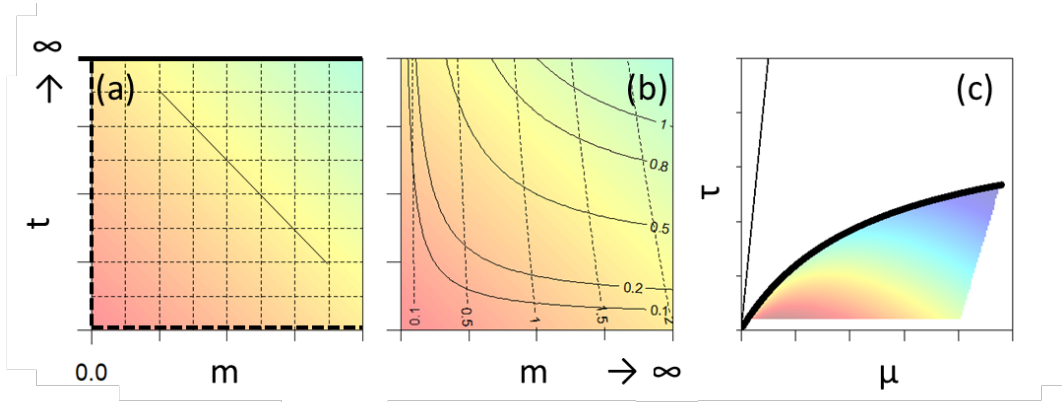


Figure 5. A time slice of the space of fluctuations at fixed clock time, showing a biological response  $R = 100 - t - m$  as a heat map. (a)  $mt$ -projection with  $mt$ -isolines given by straight lines (i.e. as a cartesian frame). In the heatmap of  $R$ , isolines (lines of indicating equal  $R$ -values) are given by diagonals (note colour gradient) and one such diagonal is shown as a continuous line. The horizontal top line represents the line at infinity corresponding to constant conditions. Dashed lines at  $m = 0$  and  $t = 0$  are open boundaries. (b)  $mt$ -projection with  $\mu\tau$ -isolines given by curves, (here taken from Case 1), with all parameters of Eq. (3) & (4) set to  $= 1$ , except  $k_\mu = 0.1$ . (c)  $\mu\tau$ -projection. The space occupied by the fluctuations is constrained to the coloured area by the maximum values of  $m$  and  $t$ ; these represent the maxima used in a realistic experiment. The thick black curve is the upper limit set by the maximum value of  $t$  and the straight line is the theoretical maximum. Isolines of equal body size (diagonals in a-b) form petal-like curves in (c) and the parabolas of (b) would give straight lines in (c).

#### 4.1 Case 1: hyperbolic model

For tolerance, I use an inverse function  $E = E(t) = 1/(S_0 + k_\mu t)$ , with  $S(t) = (S_0 + k_\mu t)$ . Here,  $S$  increases linearly with the time scale of the fluctuation, from a minimum  $S_0$  defined as  $1/T_{max}$ ; the constant  $k_\mu$  is a rate of increase. In such a case we obtain:

$$\mu = m(S_0 + k_\mu t) \quad (3)$$

In addition, I will assume that developmental time follows an inverse function of temperature, such that:

$$\tau = t(D_{min} + k_\tau/m)^{-1} \quad (4)$$

where  $D_{min}$  is the asymptotic minimum developmental time achieved, as  $m \rightarrow \infty$ , in the absence of developmental impairments.

The values of the intrinsic frame define a non-linear and non-orthogonal coordinate frame (Fig. 5b). Equations 3 and 4 define hyperbolic curves, as lines of equal  $\tau$  (or  $\mu$ ) in a similar way as the straight lines in define lines of constant  $m$  or  $t$  (Fig. 5a). Consecutive lines define areas of different size with the shape of such area depending on the constants ( $S_0$ ,  $D_{min}$ ,  $k_\mu$ ,  $k_\tau$ ) driving the tolerance and developmental time. Such lines do not meet at straight angles reflecting the fact that  $\mu$  and  $\tau$  are not mutually independent variables.

An alternative view of the response, highlighting the organismal perspective, is given by the “ $\mu\tau$ -projection” (Fig. 5c). This is analogous to the projection obtained from principal component analysis, where communities are represented as points in a space. Before the PCA is carried out, the original projection (analogue to the mt-projection here) would have species abundances as axes. The difference is that the PCA-axes are linear and orthogonal, while  $\mu\tau$ -axes, are curvilinear and non-orthogonal. Consequently, in the  $\mu\tau$ -projection, the fluctuations are constrained to a triangular region characterised by open boundaries (coloured area in Fig 5c) and with the region being set by logistical and theoretical limits (see Supplement: Section 2).

Provided with the projections defined above, and focusing on the perspective of the organism, I highlight the following points:

1. Space of existence: The region where  $\mu \leq 1$  and  $\tau \leq 1$  defines the “space of existence”, i.e. where the response  $R$  exist. This is because  $\mu > 1$  implies that the temperature is higher than the tolerance range (hence the organism collapses). In addition,  $\tau > 1$

implies that the time scale of the fluctuation is longer than the time to maturation; therefore, one cannot establish a causal relationship between biological time and the fluctuation time scale. In other examples, the space of existence will be set at  $\tau \neq 1$  (see “Discussion”).

2. Extreme event and biological definition of heatwave: extreme events (i.e. a fluctuation compromising organismal existence) are represented by the set of fluctuations defined by the curve  $\mu=1$ . Notice that such curve defines fluctuations differing in amplitude and clock time scale. If extreme events are used as a biological definition of heatwave, then such definition would differ from that based on climatology. For instance, marine heatwaves are defined as those thermal fluctuations where the temperature exceeds a fixed threshold (the 90<sup>th</sup> percentile of a temperature distribution), for 5 or more days (Hobday et al. 2016). By contrast, the definition arising from the  $\mu$ -curves does not use fixed temperature and time scales.
3. From the standpoint of the organisms, differences among fluctuations are defined by the values of  $\mu$  and  $\tau$  (not  $m$  and  $t$ ). From the extrinsic perspective, straight lines (i.e. the Euclidean distance) should define the difference (=shortest distance) between any two fluctuations (Fig. 5a; also recall the analogy to PCA for ecological communities). However, from the intrinsic perspective, the shortest distance between any two fluctuations is given by the hyperbolic curves (Fig. 5b). Hence, whether two fluctuations are experienced by the organism as very different or rather similar depends on the distance along the hyperbolic curves. In this case, the projection in the  $\mu\tau$ -plane (Fig. 5c) might give a more intuitive view of the differences among fluctuations, from the organismal perspective.
4. The invariant response (body size at maturation) is distorted as we compare the different projections (Fig. 6). The distortion reflects important biological effects of temperature on both tolerance and biological time. In the simulation (details in Supplement: Section 3), the invariant response is more sensitive to  $m$  than to  $t$  (equation in Fig. 6) but it becomes more sensitive to  $\tau$  than to  $\mu$  (compare change in colour gradient in Fig. 6a vs Fig 6b). The distortion reflects the fact that the organism will experience the response as being different from what is shown by the extrinsic frame.

Next, Case 2 uses realistic functions and highlights (by comparison to case 1) properties that are robust to changes in the mapping functions.

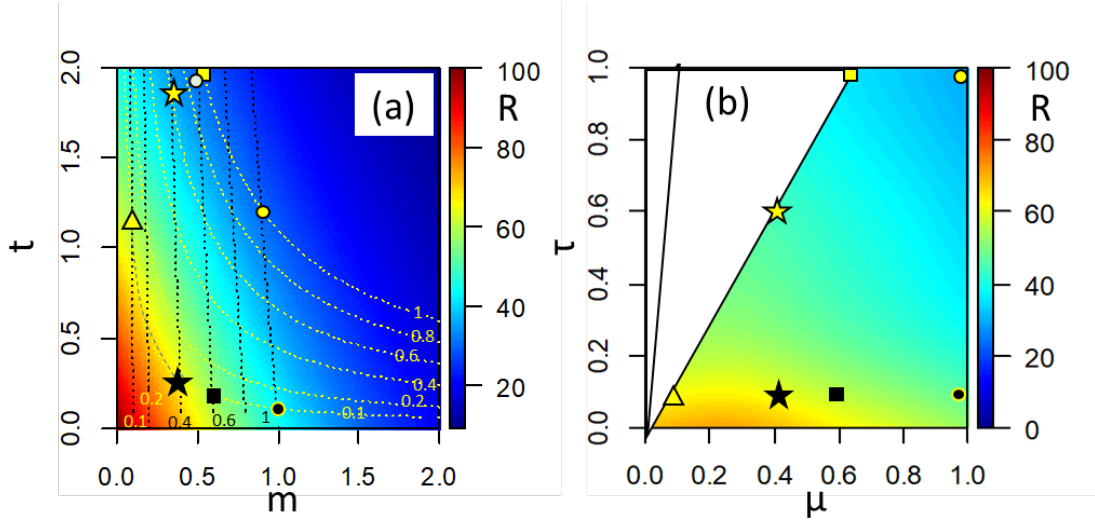


Figure 6. A time slice of the space of fluctuations at fixed clock time (a)  $mt$ -projection with intrinsic coordinate frame included: (b)  $\mu\tau$ -projection. Different symbols in (a) represent fluctuations which are shown in (b) to highlight the deformation produced by the intrinsic frame. The diagrams were constructed within the range  $(0, 2)$  for both  $t$  and  $m$ . The mapping functions are as follows: Eq. (3):  $S_0 = 1$ ,  $k_\mu = 0.1$ , Eq. (4):  $D_{min} = 1$ ,  $k_\tau = 1$ . The response was modelled as  $R = 100 \cdot \exp(-0.4m - 0.8t)$ .

## 4.2 Case 2: Combining metabolic theory and thermal tolerance

Here, I consider empirically obtained functions for developmental time and tolerance and use  $mt$ -projection to focus on the region of existence and on the definition of extreme events. Developmental time is defined in the metabolic theory of ecology of Brown (2004), such that:

$$\tau = tL_{max} \cdot e^{\frac{-A}{(m+273)}} \quad (5),$$

where  $m$  is the temperature (in  $^{\circ}\text{C}$ ),  $L_{max}$  is the inverse of the asymptotic minimum of developmental time and  $A$  is the ratio of activation energy ( $0.64 \text{ eV}$ ) and the Boltzmann constant ( $8.617 \cdot 10^{-5} \text{ eV Kelvin}^{-1}$ ).

The effect of the fluctuation is modelled following work on thermal death times (Bigelow 1921, Urban 1994, Tang et al. 2000, Rezende et al. 2014, Jorgensen et al. 2019). Those studies show that responses to temperature can be modelled with two separate functions: (1) A thermal range characterised by moderately high (or low) temperatures, where survival is independent of the exposure time. Responses in this range are equivalent to those covered in Giménez et al. (2022) where  $\mu$  is proportional to  $m$ , because  $E$  would not vary with time. (2) Beyond a thermal threshold,  $E$  decreases linearly with the logarithm of exposure time. I focus on this range, assuming that the tolerance range is proportional to the logarithm of the time scale of the

fluctuation. Here,  $E(t)$  depends on the knockout temperature ( $= M_{out}$ ) according to the equation  $M_{out} = M_{crit} - z\varepsilon_1 \log(t\varepsilon_2)$ . Here,  $M_{crit}$  is the knockout temperature corresponding to a unit of clock time ( $t = 1$ ),  $z$  is the sensitivity of  $M_{out}$  to change in  $\log(t)$ . In addition,  $\varepsilon_1$  and  $\varepsilon_2$  are proportionality constants ( $= 1$ ) and are no longer considered. By setting  $E_{max} = M_u - M_{crit}$  (maximum tolerance range), we obtain:  $E(t) = E_{max} - z\log(t)$ . In such a case the biological magnitude in the intrinsic frame ( $\mu$ ) is given by the equation.

$$\mu = \frac{m}{[E_{max} - z \cdot \log(t)]} \quad (6)$$

As in Case 1, the lines at  $\mu = 0$  and  $\tau = 0$  are open boundaries, and the lines of constant  $\mu$  or  $\tau$  are curves, representing a non-orthogonal reference frame that will also deform any invariant response (further similarities discussed in Supplement: section 4). In the mt-projection, values of  $\mu$  (heat maps in Fig. 7), capture the general pattern observed by studying thermal death times i.e., low amplitude but long period fluctuations can be as bad as high amplitude short period ones.

Case 2, based on empirical models, gives again a definition of extreme event as in Case 1, where the critical temperature defining the heatwave (here represented as  $m$ ) depends on the clock time scale of the thermal fluctuation (Fig. 7); here, the position of the curve  $\mu = 1$  depends on  $\log(t)$ . In addition, the set of extreme fluctuations and the region of existence depends on the thermal sensitivity ( $z$ ) and the maximum tolerance range ( $E_{max}$ ). At high  $z$  and narrow  $E_{max}$  (Fig. 7a), the region of existence is constrained to fluctuations that are shorter than the time to maturation ( $\tau = 1$ ). In the simulation, there is only a narrow region ( $t > 30$  in Fig. 7a) where the curve of the extreme fluctuations ( $\mu = 1$ ) is located to the right of the curve of  $\tau = 1$ . This indicates that extreme fluctuations occur at time scales longer than the time to maturation. At other combinations (Fig. 7b-d) such region expands; for instance, for  $z = 1$  and  $E_{max} = 35$ , most of the extreme fluctuations occur at time scales that are longer than time to maturation (Fig. 7d).

It is important to note that the interpretation of the isolines  $\mu = 1$  and  $\tau = 1$  depends on the specific case. For example, it may not be possible to quantify tolerance beyond maturation, i.e. in the region located to the right where  $\tau > 1$  (the maximum time scale covered in the experiment). Likewise, in the region where  $\mu > 1$ , developmental time cannot be quantified. However, tolerance may be quantified in the region where  $\tau > 1$  in the case of e.g., a multigenerational study where the biological time is defined as generation time. In an example of organisms growing to metamorphosis (instead of maturation), scenarios where the curve  $\mu$

$\tau = 1$  is located to the right of  $\tau = 1$  would indicate that reaching a critical life history stage (e.g. metamorphosis) has the potential to “rescue” the organism (or population) from the consequences of an extreme fluctuation. For species experiencing metamorphosis and habitat shifts, thermal conditions before the shift may not be the same as in the post-shift habitat. Alternatively, organisms may experience shifts in capacity to tolerate increased temperatures, for instance in association to a metamorphosis: larval stages are usually more sensitive than juveniles and adults (Pandori & Sorte 2019). In both cases, reaching metamorphosis would be analogous to reaching a thermal refuge. In semelparous species, reaching maturation and reproduction ( $\tau = 1$ ) is central, but post-reproductive life ( $\tau > 1$ ) is of no relevance for fitness. In any case, SOFiA captures important aspects of ontogeny, physiology, and phenology as drivers of responses to extreme events.

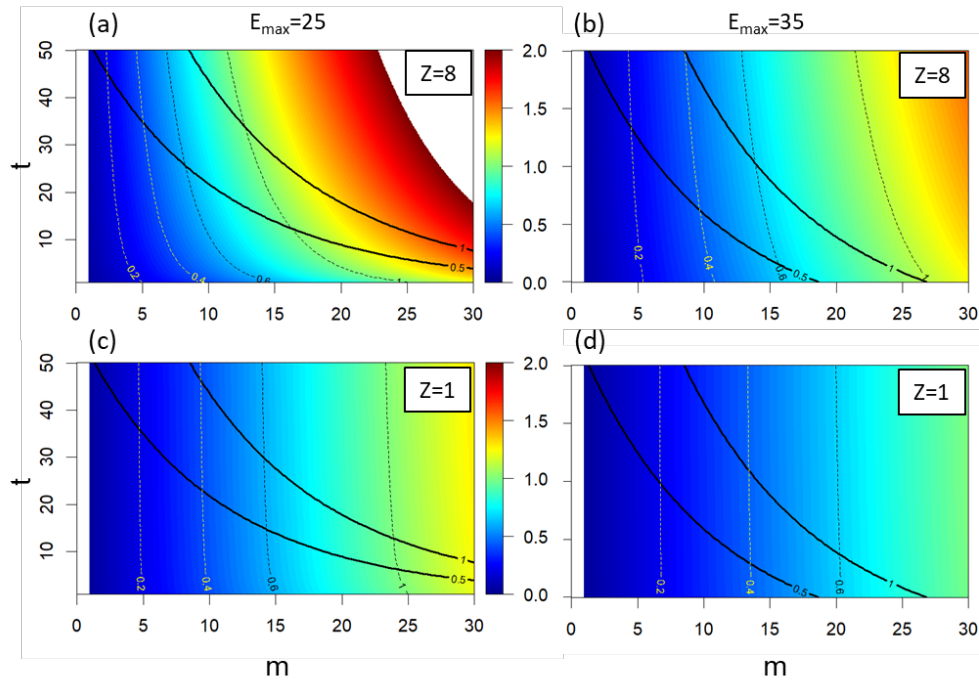


Figure 7. Case 2: A time slice of the space of fluctuations at fixed clock time showing a heatmap of  $\mu$  based on equation 6. Each panel has different values of  $z$  and  $E_{\max}$  (i.e. tolerance range at  $t = 1$ ). Dashed lines are selected lines of constant  $\mu$ : note that at small  $z$ ,  $\mu$  becomes proportional to  $m$  and less dependent on  $t$ . Continuous lines are lines of constant  $\tau$  (Eq. 6,  $L_{\max} = e^{22.47}$ ).

### 4.3 Case 3: Role of adaptive plasticity

In the above cases, the tolerance depended only on the time scale of the fluctuation. However, the presence of adaptive plasticity should (within limits: DeWitt et al. 1998) either shift or expand the tolerance range (Angiletta 2009, chap. 5; Seebacher et al. 2014, Salachan et al. 2022) in response to the (thermal) fluctuation. We can visualize the rescue effect of adaptive plasticity as an expansion of the space of existence in the  $mt$ -representation (see below).

Plasticity involves three main steps (Windig et al. 2004); i.e. where (1) a cue is converted to a signal (e.g. hormones: Duffy et al. 2002) that (2) triggers a change in the phenotype which results in (3) a change in its performance (= tolerance). Those steps lead to a latency period (Laubach et al. 2022) between the moment when an environmental cue is detected and when the phenotype is functional. The latency period varies according to the type of plasticity: from short (hardening: Hoffmann et al. 2003), through developmental (Salachan and Sorensen 2017) to transgenerational plasticity (Donelson et al. 2012). The relationship between the latency period and the time scale of the fluctuation may range between two extremes. On one extreme, the fluctuation may be perceived as a short-term pulse with respect to such period (Manenti et al. 2018) while on the opposite extreme the fluctuation is perceived as a long period wave. In the first case, the tolerance range depends on whether the organisms (or the parents) experienced a previous fluctuation. In such a case, we may define the acclimation state of an organisms as  $E_i(t)$  which will shift from  $E_1(t)$  to  $E_2(t)$  after a fluctuation is experienced. One may model such change of state as a change in the parameters defining the equations of case 2 (previous section).

I focus on the case (Fig. 8) where the latency period can be much shorter than  $t$  so that (1) the acclimation state changes as the fluctuation is experienced and (2) the fluctuation can be sufficiently long to alter developmental time. An example is the acclimation to seasonal fluctuations in temperature where organisms acclimate to summer (or winter) conditions well in advance of the time of maximum (or minimum) temperatures. I model those steps through functional responses, with the overall result that changes in the cue (temperature) are mapped into changes in the thermal tolerance and  $\mu$  (Fig 8). This simulation differs from cases 1 and 2 in that here I modelled the time course of the response (details in Supplement: section 5). I do not intend to develop a mechanistic model (see e.g. Hazel et al. 1990, Buoro et al 2012) and I must emphasise that the model is intended as illustration of how plasticity can be incorporated to SOFiA.



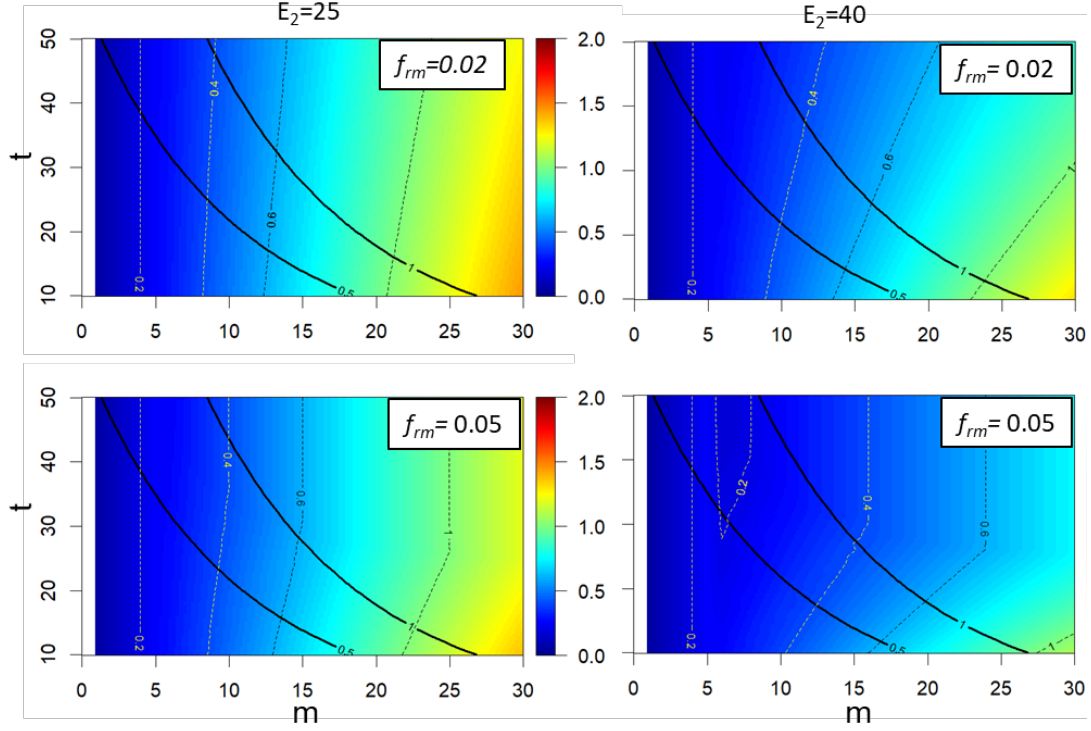


Figure 8. Case 3, Adaptive plasticity: A time slice of the space of fluctuations at fixed clock time showing a heatmap of  $\mu$ . Different panels (a-d) show  $\mu$  for different values of maximum tolerance range ( $E_2 = 25$  and  $E_2 = 40$ ) expanded from a value of  $E_2 = 20$  before the fluctuation is experienced. The inset values correspond to the maximum rate of phenotypic change ( $=f_{rm}$ ) as driven by temperature (equations in Supplement, Section 5). In all panels, the signal activation threshold was at  $5^\circ\text{C}$ : this is best noted at  $E_2 = 40$  and  $r_{max} = 0.05$ . Continuous lines: constant  $\tau$ -values; dashed lines: constant  $\mu$ -values.

The rescue effect of adaptive plasticity is shown as the expansion of the region of existence: the curve  $\mu = 1$  is shifted to the right (as compared to Cases 1 and 2). Hence, the rescue effect is manifested in the set of fluctuations defining extreme events. As compared to the previous cases, extreme events occur at high values of  $m$ . The region where the plastic response operates depends on the three main steps: (1) The threshold response to the cue: below some thermal threshold (fixed to  $5^\circ\text{C}$  in Fig. 8 and  $10^\circ\text{C}$  in the supplement, Fig. S4) the plastic response is not triggered ( $m < 5^\circ\text{C}$  in Fig. 8). The tolerance range is still wide (giving low  $\mu$  values). In the model, the threshold response is driven by the thermal threshold  $y_u$  of the first functional response:

$$F_{c \rightarrow s} = \frac{1}{1 + e^{k_s[y_u - y(x)]}} \quad (7)$$

where  $F_{C \rightarrow S}$  is the function converting a cue to a signal,  $y(x)$  is the temperature fluctuating through clock time ( $=x$ ) and  $k_S$  is a rate constant indicating how sharp is the triggering of the response.

(2) The rate of phenotypic change in response to temperature  $f_r$ :

$$f_r = \frac{f_{rm} \cdot y}{k_r + y} \quad (8),$$

where  $f_{rm}$  is the maximum rate of phenotypic change and  $k_r$  is the half saturation constant in the model; the inverse of  $f_{rm}$  is time scale, defined here as the minimum latency period.

This rate is the component of the second functional response:

$$F_{S \rightarrow P} = f_{sp1} + \sum_x f_r(x) \quad (9)$$

$F_{S \rightarrow P}$  maps the signal to the phenotypic state (as a continuous variable) from an initial state,  $f_{sp1}$  (before the signal activates the response) up to an upper threshold  $= f_{sp2}$ , remaining constant thereafter. Because Eq. (9) has an asymptotic maximum ( $f_{rm}$ ), the rate of phenotypic change is constrained; in consequence, if the time scale of the fluctuation is sufficiently short, there is no sufficient time for the plastic response to reach its maximum value. Hence, plasticity operates on the  $\mu$  values at intermediate values or  $m$  and  $t$  (at moderately high  $m$ ).

(3) The maximum thermal tolerance range, defined in the third functional response of the model,  $F_{C \rightarrow S}$ , which maps the phenotype to the thermal tolerance. This function is linear between the lower ( $= E_1$ ) and the upper tolerance range ( $= E_2$ ) and defines the region of existence in Figure 8.

#### 4.4 Worked example

The worked example (Fig. 9, details in Supplement: Section 6, and data files) represents an experiment aimed at (1) quantifying the effect of the magnitude and time scale of thermal fluctuations on the body size of a marine ectotherm and (2) estimating the average body mass, given a set of fluctuations of varying magnitude and time scale. The example represents experiments taking place over several weeks to few months, which corresponds to those carried out with short lived organisms (e.g. copepods) or a specific life phase of a long lived species (e.g. larvae). Biological time is referred up to maturation (copepods) or metamorphosis (fish or invertebrate larvae). In both cases, temperature has a strong effect of developmental time (copepods: Guerrero et al. 1994, McLaren 1995; marine larvae: O'Connor et al. 2007); hence, the functions mapping the time coordinates are important. For example, within species

increased temperature can reduce larval developmental time by 50% over the tolerance range, which can span 10-15°C (but varies among species: O'Connor et al. 2007). Increases of only 3°C can have important reductions in developmental time towards the lower sector of the thermal tolerance range: for example, in one of the best studied crustaceans, the shore crab *Carcinus maenas* an increase in temperature of 3°C reduces the larval developmental time (to megalopa or first crab stage) by a 25 to 35% within the range 12-18°C, corresponding to summer temperatures in the distribution range (Dawirs 1985, DeRivera 2007, Šargač et al. 2022). The functions mapping time coordinates become more important at that sector, especially under long fluctuation time scales. At the upper sector of the thermal tolerance range, biological time is little affected by temperature; however, at that sector, the functions mapping from the extrinsic to intrinsic magnitude coordinates should become important if tolerance depends on the time scale of the fluctuation.

The experiment follows a gradient design (Kreyling et al. 2018) with 10 levels of thermal magnitude crossed with 9 levels of time scales, giving 90 locations (i.e. combinations of time scales and magnitudes) in the space of fluctuations. Organisms are observed every day in order to record the time at maturation and the time at which they reach the thermal limit (i.e. they die or exhibit a predefined behavioral response). In the first step, non-linear regression models are used to obtain the equations giving the  $\tau$ ,  $\mu$ , size after 70 days of experiment,  $R_1(m, t, t^* = 70 \text{ days})$ , and size at maturation  $R_2(m, t, \tau^* = 1)$ . For the second objective, the functions  $R_1$  and  $R_2$  are used to estimate the average response through scale transition theory, model simulations and the so-called mean field approach.

The constraint on the number of times at which size can be observed reproduces a realistic experiment where animals die beyond the region of existence and where measurements of body size is too invasive to be performed more than twice or where there are logistical constraints. With some caveats (see next paragraph) the example may also be taken as a case study of a species monoculture (e.g. macroalgal or mussel bed) or natural community, recovering after a disturbance event, where the biological variables are generation time (or the inverse of species replacement rate), tolerance (or species richness) and biomass (or some ecosystem service).

In the worked example, the curves  $\mu = 1$  and  $\tau = 1$  cross each other as expected if some of the fluctuations enable maturation, but others kill organisms before reaching maturity. In other situations, such curves may not cross, but the experiment will still provide valuable information. If all animals reach maturity, the experiment will quantify the dependence on body

size on the time coordinate frame. If by contrast, thermal thresholds are reached before maturation, the experiment would provide information about the region of existence and identify the set of fluctuations defined as extreme (i.e. the set defined by the curve  $\mu = 1$ ).

The importance of the mapping function is given by the following points. First, the function  $\tau^*(m, t, t^*)$ , mapping coordinates of observation time, shows that responses differ considerably depending on whether we quantify size at maturation or at a given clock time. The difference is shown in maps of figure 9 (contrast Figs. 9a-b vs 9c) and in the estimated body size given an average heatwave (Table 1: compare  $R_1$  vs  $R_2$ ). Second, the function  $\mu(m, t)$ , quantifies the effect of the time scale of the fluctuation on thermal tolerance; it predicts which heatwaves would result in system collapse: this is illustrated in Figure 9b as the white area, which corresponds to heatwaves with combinations of magnitudes and time scales ( $m$  and  $t$  coordinates) leading  $\mu(m, t)$ . Third, the combination of the above-mentioned functions predicts the set of heatwaves still enabling animals to be “rescued” by achieving maturity (or metamorphosis): this is illustrated in Figure 9b as the portion of the curve  $\tau^* = 1$  lying at the left of the curve  $\mu = 1$  (i.e. not in the white area). Fourth, the combination of  $\mu(m, t)$  and  $\tau(m, t)$  predicts the set of fluctuations of a time scale equal than the time to maturation (or to metamorphosis) are not tolerated. This is illustrated in Figure 9b the curve  $\tau = 1$  (dashed line) lying at the right of the curve  $\mu = 1$ , if  $m > 5$ ; the portion lying at the left of the curve  $\mu = 1$  is predicted to occur if larvae experience fluctuations of time scales larger than 50 days.

In interpreting  $R_1$  and  $R_2$  (Figs 9b, c) one must recall that such functions are on different surfaces that cut the volume representing the time course of the invariant response (Fig 3). The difference between  $R_1$  and  $R_2$  (Fig. 9b, c) is carried out by the modelling of the average response (Table 1) to a set of fluctuations (Fig. 9c), but in both  $R_1$  and  $R_2$ , the mean field approach underestimates the average response as compared to simulating from the model or applying scale transition theory.

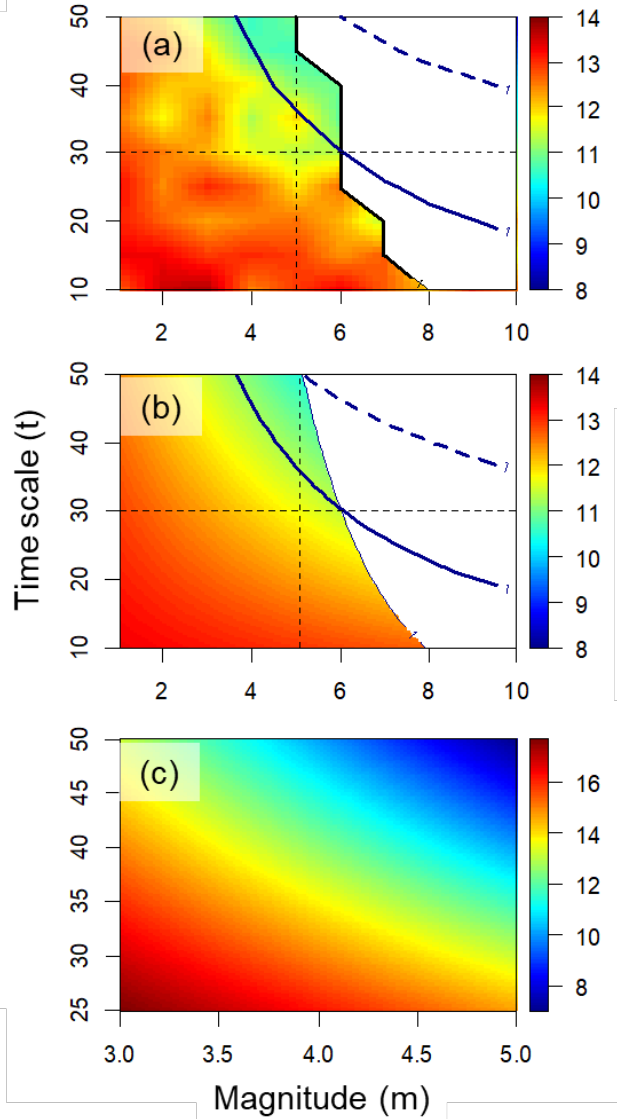


Figure 9. Worked example. Simulation of an experiment quantifying the role of magnitude and time scale of thermal fluctuations on body size (color heatmap) of a marine organism at maturation. (a) mt-projection of the observed response at a fixed clock time ( $t^* = 70$  days). (b) Fitted curves and body size at the same fixed clock time as in (a). (c) mt-projection of the fitted response at maturation. The projections in (a) and (b), correspond to a flat time slice (see Fig 3): the  $\mu = 1$  curve is the black line delimiting the white area (i.e. no data at  $\mu > 1$ ). The curve of the time at maturation,  $\tau^* = 1$ , is given as a continuous blue line; the dashed blue line corresponds to the curve of  $\tau = 1$  (fluctuation with time scales of the maturation time). The curves of  $\tau^*$  and  $\tau$  differ because they are scaled to different time variables. The vertical dashed line delimits the region (to the left) where maturation is reached irrespective of the time scale of the fluctuation. The horizontal dashed line delimits an upper region where maturation can be reached. The heatmap in (c) lies on a curved surface (see Fig. 3) and it is restricted to the region of the space of fluctuations enabling maturation (note axis ranges). The data (csv file) and procedures are given in Supplement, Section 6.

Table 1. Estimated body size (in arbitrary units) at  $t^* = 70$  days ( $R_1$ ) and at maturation ( $R_2$ ) based on mean field approach, scale transition theory and model simulation.

	$R_1$	$R_2$
<b>Mean field</b>	11.95	14.12
<b>Scale transition</b>	11.92	14.03
<b>Simulation</b>	11.92	14.03

## 5. DISCUSSION

Here, I presented a geometric approach (SOFiA) to understand biological responses to temperature (or other environmental fluctuations), from the perspective of organisms. This approach expresses the organismal perspective as a coordinate frame within a space defined by fluctuation components and the times at which observations are made in an experiment. Using temperature as example, I showed how this approach ingrates our current knowledge about effects of environmental variables on organisms. We know that temperature has strong non-linear effect on biological time (McLaren 1995, Gillooly et al. 2001); that thermal tolerance decreases non-linearly with the exposure time (Rezende et al. 2014), and that adaptive plasticity has a characteristic time course (Windig et al. 2004). The organismal perspective is obtained from the relationship between different types of biological traits: (1) traits driving tolerance and biological time provide the metric for the biological scaled magnitude and time of a fluctuation. (2) There are traits, called invariant responses, responding to tolerance and biological time. (3) Traits defined by rates are identified as those with magnitude depending on the reference frame. In addition, the geometric approach presented here highlights the importance of considering the frame used to scale the time at which observation are made because of its consequences in the observed invariant response. The result is the capacity to quantify biological responses in different frames which should lead to better mechanistic understanding; in addition, the approach presented here is able to provide predictions for field conditions (through e.g. scale transition theory: as shown in the worked example).

A main feature of SOFiA is the mathematical formalism, represented by a set of functions and partial differential equations. One may argue that this is merely a formalizing exercise only providing more precision. However, the mathematical formalism is central to identify counter-intuitive results arising from interactive effects and non-linearities. A similar approach has helped to identify the conditions where interactive effects, occurring at a level of organization (e.g. individuals), are not mapped into a higher level of organization (population: DeLaender 2018). Likewise, the mathematics of scale transition theory (Denny & Benedetti-Cecchi 2012) is needed to determine when (and in what extent) the average of the biological response does not match the response to the average temperature. In all those cases quantitative predictions are not those expected from intuition. The approach presented here deals with non-linearities and interactive responses to the predictors (as above), and non-linear transformations between different frames. For example, the solutions of partial differential equations can help us to identify scenarios when the type of multiple driver response depends on the metrics of time

(worked example, Fig. 9 and Giménez et al. 2022). Given only two components of a single fluctuation (magnitude and time scale) we can still rely on 2D graphical representations for a better understanding of a response depends on the coordinate frames, as illustrated Figure 3 (i.e. the response on different surfaces). However, in cases of two or more fluctuations (e.g. temperature plus a second environmental variable) the responses will lie on higher dimensional surfaces and intuition will be of limited help. It seems to me that, as the field progresses, the stronger mathematical emphasis will constitute an important guide to navigate through the complexity of high dimensional phenomena, interactive effects and non-linearities. Hence, the mathematical analysis used here, may be considered an additional step in the processes summarised in Figure 2, helping with the design and interpretation of experiments as well as the application scale transition.

SOFiA incorporates the biological perspective, defined by the time scale and the capacity of organisms and other biological systems to cope with environmental fluctuations. The first important concept is the “region of existence”, defined from fixed values of  $\mu$  and  $\tau$  (both set to 1 in the example). This is an important point in the light of discussions concerning the definition of heatwaves (Baley and Van de Pol 2015, Hobday et al, 2016, Jacox 2019). From the biological standpoint, heatwaves would be defined as the set of extreme fluctuations (characterised by  $\mu = 1$ ), which depend on the time scale of the fluctuation. Many studies show that tolerance to a given stressor scale with the inverse of the logarithm of the time of exposure (revision in Rezende et al. 2014). Such biological definition would incorporate the rescue effect produced by adaptive plasticity. Simulations in Case 3 highlight the importance of time delays in the expression of the plastic response in determining the set of extreme fluctuations.

The starting point in SOFiA was to consider fluctuations as a collection of components (as in Hobday et al. 2016) and defining fluctuations as objects existing in an hypervolume, in the same way that ecologists define elements in the ecological niche (Blonder 2018) or characterise communities (e.g. Legendre & Legendre 2008). At the organismal level, the space of fluctuations has connections with the concept of tolerance landscape (Rezende et al. 2014) where the response is tolerance, as existing within a space defined by the magnitude and time scale of exposure to a particular stressor. At the species level, there are connections with the Hutchinson view of the niche (i.e. where resources or environmental variables define the axes), but adding time variables, and meeting the needs of incorporating phenology into the concept of the niche (see Ponti & Sanolo 2022). In addition, for both cases, the main contribution of

SOFiA is the quantification of the perspective of organisms through additional reference frames.

Different perspectives, including that of the observer, are related through mapping functions (from  $t$  to  $\tau$  and  $m$  to  $\mu$ ). We can also consider a case with two different frames representing two different species; in such a case, we can remove the reference frame of the human observer from the equations (see Supplement: Section 7) and project the response of the first species from the perspective of second one. The framework can also be used to visualise biological responses underpinned by different mechanisms (or based on empirical fits) of how tolerance and biological time respond to a given fluctuation. For example, the comparison among cases 1- 3 helps to identify properties that are contingent on the presence of plasticity or the adoption of a specific type of trade-off between critical temperature of tolerance period. In addition to the metabolic theory of ecology, the response of developmental time has been predicted from theory or other equations (Ahlgren 1987, Guerrero et al. 1994, McLaren 1995, Shi et al. 2016, Quinn 2021).

In SOFiA, the rescue effect of adaptive plasticity (Windig et al. 2004, Chevin et al. 2010) is expressed as the expansion the region of existence (where effects of fluctuations on invariants are buffered). In the simulation, the expansion occurred at intermediate time scales because short term thermal fluctuations were not enough to sustain rapid phenotypic change. Expansions of the space of existence at shorter (or longer) time scales should be based on the concerted action of plastic responses operating at different time scales, i.e. from hardening to long term acclimation (Donelson et al. 2011). Hence, the simulation shows that better understanding of the responses to fluctuations requires models of the “dynamics” of the formation of the phenotype, which instead will depend on the scale-dependent plastic response. Such models require experiments quantifying how the rate of phenotypic change experienced by an organism is driven by temperature; central to such research are time keeping mechanisms (Giménez et al. 2022) and metabolic rates (Jackson et al. 2021).

An important point in SOFiA is to differentiate between invariants (e.g. body mass) and rates (e.g. growth or sensitivity). Rates capture the relative aspect of the “effect” of a fluctuation on the invariant because they depend on the reference frame. Hence, SOFiA introduces a level of “relativism” in the nature of the responses to stressors. This is particularly important when more than one stressor is considered. In such a case, the type of frame (intrinsic or extrinsic) determines the nature of the interactive effect of two stressors on an invariant response



(Giménez et al. 2022). An important example concerns the combined effect of increased temperature and a second environmental variable. For instance, because temperature increases metabolic demands, increased temperature can exacerbate the negative effect of food limitation on body reserves to metamorphosis (Torres & Giménez 2020). In addition, increased temperature can either mitigate or exacerbate the effect of reduced salinity on survival to metamorphosis (Torres et al. 2021). Importantly, because thermal fluctuations drive developmental rates, the magnitude of body size responses can be only expressed as relative to the reference frame used to measure time. The relativism introduced here has implications for multiple stressor research; for instance, additive effects relative to the clock time will become interactive in biological time (Giménez et al. 2022). Multiple stressor research has been motivated by the recognition that climate change affects several environmental variables at a time (Gunderson et al. 2016, Boyd et al. 2018). An important objective of this field involves the quantification of the frequency of occurrence of the different types of interactive effects and in which context a stressor mitigates or enhances the effect of another stressor. The fact that the nature of the multiple stressor effect can depend on the reference frame highlights the need to be clear about what is the relevant frame to address a given question.

## 5.1 Wider applications

I argue that SOFiA is a general approach in the following sense. First, it can be applied in situations where biological time and tolerance do not depend on the fluctuations or to more complex experimental designs. If biological time and tolerance do not depend on the fluctuation, the partial differential equation 2 simplifies such that the matrix  $M$  contains zero's in the off-diagonal entries ( $\mu$  and  $\tau$  become linearly related to  $m$  and  $t$  respectively) and the response is projected on 2D flat time slices (Fig 3) at both clock and biological time. Second, given a single variable (e.g. temperature), one can apply this approach to experiments exploring the effect of consecutive waves on biological variables responses, by adding a component (to the space of fluctuations) quantifying the time lag between waves (called respectively  $l$  and  $\lambda$  in the extrinsic and intrinsic frames). Third, one can accommodate additional variables (e.g. food availability, salinity,  $pCO_2$ ) and the time lag among them, in order to explore the effect of simultaneous vs sequential stressor effects (Gunderson et al. 2016). As the level of complexity increases, the limitations are logistical; however, in such a case, one could use information from previous experiments and the mathematical formalism to determine which region of the space of fluctuations should be further explored through a new experiment. Fourth, SOFiA can

be applied beyond the organismal level, if one can define metrics for biological times and tolerance (discussion below).

A potential application concerns the species level, where tolerance may be defined as the thermal range enabling positive population growth rate (Gvozdk 2018) and biological time is defined as the generation time. Given two species, we have species-specific biological time scales ( $\tau_1, \tau_2$ ) and amplitudes ( $\mu_1, \mu_2$ ). In the mt-projection, the area where both  $\mu_1$  and  $\mu_2 > 1$  are regions of extinction for both species. The regions where only one of them is  $> 1$ , shows extinction of only one such species; interactions such as symbiosis would be reflected as  $\mu_1 = \mu_2$ . Areas where any  $\mu_i > 1$  indicate conditions leading to environmental filtering (Kraft et al. 2014) where temperature selects for species assemblages characterised by specific traits combinations. How  $\mu_i = 1$  curves are positioned with respect to  $\tau_i = 1$  curves will define regions where extreme fluctuations are longer/shorter than the generation times. Theory (Romero-Mujalli et al. 2021) predicts that the threshold of  $\tau = 1$  is important for how adaptive plasticity responds to fluctuations over long time scales.

Portfolio effects (Schindler et al. 2015), driven by phenotypic plasticity and genetic diversity, buffer populations from environmental fluctuations. Portfolio effects should result in patterns analogous to those of Figure 8, which contrast to those shown in Figure 7. There are also outcomes that depend on the type of interaction. In case of competition, relative nonlinearity and storage effects maintain coexistence under environmental fluctuations (Descamp-Julien & Gonzalez 2005, Chesson 2018); fluctuations of sufficiently low amplitude should result in competitive exclusion, unless fluctuation independent mechanisms operate. Fluctuation-dependent mechanisms may be reflected in  $\mu$ -values if “tolerance” is quantified considering the outcome of species interactions.

The second case concerns biodiversity and ecosystem function (Garcia et al. 2018), where the invariant function would be biomass or the amount of habitat produced by a foundation species. Examples are macroalgal or mussel beds and coral reefs sustaining function in association to its biomass or canopy. Increases in temperature lead to e.g. coral bleaching (Pratchett et al. 2008). Here, the curve  $\tau = 1$  would represent fluctuations occurring at the time scale of the species replacement (i.e. a metric of biological time unit at the level of community: Ontiveros et al. 2021). Community tolerance is defined from the sensitivity of species richness to changes in the time scale of the fluctuation. By moving along the line of  $\mu = 1$ , we can identify the set of environmental fluctuations driving extinction and collapsing the function. The absence of

buffering mechanisms should result in patterns like Figure 7. Buffer effects (as plasticity in Fig. 8) will reflect phenotypic plasticity, portfolio, or storage effects. In addition, at this level, species complementarity should also operate as a buffer; species complementarity can sustain function in scenarios of increased temperature (Garcia et al. 2018).

In synthesis, SOFiA could help to advance our understanding and to predict effects of environmental fluctuations on biological systems. This is achieved through the synthesis, organisation, and re-interpretation of current information about effects of environmental fluctuations on tolerance, biological time and chosen “invariant” responses. As a perspective, SOFiA offers a route for future research, combining a mathematical analysis, simulations and experiments (manipulating fluctuation components) which are then integrated in a wider research programme.

## REFERENCES

- Abram, PK, Boivin G, Moiroux J, Brodeur J (2017) Behavioural effects of temperature on ectothermic animals: unifying thermal physiology and behavioural plasticity. *Biol Rev* 92: 1859–1876.
- Ahlgren G (1987) Temperature functions in biology and their application to algal growth constants. *Oikos* 49:177–190.
- Angilletta MJ (2009) *Thermal adaptation: a theoretical and empirical synthesis*. Oxford.
- Bailey LD, van de Pol M (2016). Tackling extremes: challenges for ecological and evolutionary research on extreme climatic events. *J Anim Ecol* 85:85–96.
- Benedetti-Cecchi L (2003) The importance of variance around the mean effect size of ecological processes. *Ecology* 84: 2335–2346.
- Benedetti-Cecchi L (2021) Complex networks of marine heatwaves reveal abrupt transitions in the global ocean. *Sci Rep* 11:1739.
- Benedetti-Cecchi L, Bertocci I, Vaselli S, Maggi E (2006). Temporal variance reverses the impact of high mean intensity of stress in climate experiments. *Ecology* 87:2489–2499.
- Bernhardt JR, O'Connor MI, Sunday JM, Gonzalez A (2020) Life in fluctuating environments. *Phil Trans R Soc B* 375:20190454.

956 Bertoci I, Vaselli S, Maggi E, Benedetti-Cecchi, L (2007) Changes in temporal variance of  
 957 rocky shore organism abundances in response to manipulation of mean intensity and temporal  
 958 variability of aerial exposure. *Mar Ecol Prog Ser* 338:11-20.

959 Bigelow WD (1921). The logarithmic nature of thermal death time curves. *J Infectious*  
 960 *Diseases* 29:528–536.

961 Blonder B (2018). Hypervolume concepts in niche- and trait-based ecology. *Ecography* 41:  
 962 1441–1455.

963 Box GEP, Wilson KB (1951). On the experimental attainment of optimum conditions. *J R*  
 964 *Stat Soc B* 13:1–38.

965 Boyd PW, Collins S, Dupont S, Fabricius K, Gattuso J-P, Havenhand J, Hutchins DA,  
 966 Riebesell U, Rintoul MS, Vichi M, Biswas H, Ciotti A, Gao K, Gehlen M, Hurd K, Kurihara  
 967 H, McGraw KM, Navarro JM, Nilsson GE, Pasow U, Pörtner H-O (2018). Experimental  
 968 strategies to assess the biological ramifications of multiple drivers of global ocean change—A  
 969 review. *Glob Change Biol* 24:2239–2261.

970 Brown JH, Gillooly JF, Allen AP, Savage M, West GB (2004). Towards a metabolic theory  
 971 of ecology. *Ecology* 85:771–1789.

972 Buoro M, Giménez O, Prévost E (2012). Assessing adaptive phenotypic plasticity by means  
 973 of conditional strategies from empirical data: the latent effect threshold model. *Evolution*  
 974 66:996–1009.

975 Burraco P, Orizaola G, Monaghan P, Metcalfe NB (2020) Climate change and ageing in  
 976 ectotherms. *Glob Change Biol* 26:5371–5381.

977 Cadotte MW (2013). Experimental evidence that evolutionarily diverse assemblages result in  
 978 higher productivity. *Proc Natl Acad Sci USA* 110:8996–9000.

979 Cayuela H, Lemaître JF, Muths E, McCaffery RM, Fretey T, le Garff B, Schmidt BR,  
 980 Grossenbacher K, Lenzi O, Hossack BR, Eby LA, Lambert BA, Elmberg J, Merila J, Gippet  
 981 JMW, Gaillard JM, Pilliod DS (2021). Thermal conditions predict intraspecific variation in  
 982 senescence rate in frogs and toads. *Proc Natl Acad Sci US* 118:e2112235118.

983 Chave J (2013). The problem of pattern and scale in ecology: what have we learned in 20  
 984 years? *Ecol. Lett* 16:4–16.

985 Chesson P (2018). Updates on mechanisms of maintenance of species diversity. *J Ecol* 106:  
986 1773-1794.

987 Chevin LM, Lande R, Mace GM (2010). Adaptation, plasticity, and extinction in a changing  
988 environment: towards a predictive theory. *PLoS Biol* 8:e1000357.

989 Cottingham KL, Lennon JT, Brown BL (2005). Knowing when to draw the line: designing  
990 more informative ecological experiment. *Frontiers Ecol Environ* 3:145–152.

991 Dal Bello M, Rindi L, Benedetti-Cecchi L (2017). Legacy effects and memory loss: how  
992 contingencies moderate the response of rocky intertidal biofilms to present and past extreme  
993 events. *Glob Change Biol* 23:3259–3268.

994 Dawirs RR (1985) Temperature and larval development of *Carcinus maenas* (Decapoda) in  
995 the laboratory; predictions of larval dynamics in the sea *Mar Ecol Prog Ser* 24: 297–302.

996 Dawson TP, Jackson S, House J, Prentice IC, Mace GM (2011). Beyond predictions:  
997 biodiversity conservation in a changing climate. *Science* 332:53–58.

998 De Laender F (2018). Community- and ecosystem-level effects of multiple environmental  
999 change drivers: Beyond null model testing. *Glob Change Biol* 24:5021–5030.

1000 DeRivera C, Hitchcock NG, Teck SJ, Steves BP, Hines AH, Ruiz GM (2007) Larval  
1001 development rate predicts range expansion of an introduced crab. *Mar Biol* 150: 1275–1288.

1002 DeWitt TJ, Sih A, Wilson DS (1998). Costs and limits of phenotypic plasticity. *Trends Ecol*  
1003 *Evol*, 13:77–81.

1004 Denny M (2019) Performance in a variable world: using Jensen’s inequality to scale up from  
1005 individuals to populations. *Conserv Physiol* 7:coz053. 1.

1006 Denny M, Benedetti-Cecchi L (2012) Scaling up in ecology: Mechanistic approaches. *Annu*  
1007 *Rev. Ecol Evol Syst* 43:1–22.

1008 Descamps-Julien B, Gonzalez A (2005). Stable coexistence in a fluctuating environment: an  
1009 experimental demonstration. *Ecology* 86:2815–2824.

1010 Donelson JM, Salinas S, Munday PL, Shama LNS (2018). Transgenerational plasticity and  
1011 climate change experiments: Where do we go from here? *Glob Change Biol* 24:13–34.

1012 Dowd WW, King FA, Denny MW (2015) Thermal variation, thermal extremes and the  
1013 physiological performance of individuals. *J Exp Biol* 218:1956–1967.

1014 Fraterrigo JM, Rusak JA (2008) Disturbance-driven changes in the variability of ecological  
1015 patterns and processes. *Ecol Lett* 11:756–770.

1016 García FC, Bestion, E, Warfield R, Yvon-Durocher G (2018). Changes in temperature alter  
1017 the relationship between biodiversity and ecosystem functioning. *Proc Natl Acad Sci USA*,  
1018 115:10989–10994.

1019 Gerhard M, Koussoroplis AM, Raatz M, Pansch C, Fey SB, Vajedsamiei J, Calderó-Pascual  
1020 M, Cunillera-Montcusí D, Juvigny-Khenafou NPD, Polazzo F, Thomas PK, Symons CC,  
1021 Beklioğlu M, Berger SA, Chefaoui RM, Ger KA, Langenheder S, Nejstgaard JC, Ptacnik R,  
1022 Striebel M (2023) Environmental variability in aquatic ecosystems: Avenues for future  
1023 multifactorial experiments. *Limnol Oceanogr Letters* 8:247–266.

1024 Gerken AR, Eller OC, Hahn, DA, Morgan TJ (2015). Constraints, independence, and  
1025 evolution of thermal plasticity: Probing genetic architecture of long- and short-term thermal  
1026 acclimation. *Proc Natl Acad Sci USA* 112:4399–4404.

1027 Gillooly JE, Charnov EL, West GB, Savage VM, Brown JH (2002) Effects of size and  
1028 temperature on developmental time. *Nature* 417:70–71.

1029 Giménez L, 2006. Phenotypic links in complex life cycles: conclusions from studies with  
1030 decapod crustaceans. *Int Comp Biol* 46, 615–622.

1031 Giménez L (2011). Exploring mechanisms linking temperature increase and larval  
1032 phenology: The importance of variance effects. *J Exp Mar Biol Ecol* 400: 227–235.

1033 Giménez L (2020) Phenotypic plasticity and phenotypic links in larval development. Chapter  
1034 13 in Thiel M, Anger K, Harzsch S, Chapter in *Larval Biology*; Volume 7 of Series: The  
1035 Natural History of the Crustacea. Oxford

1036 Giménez L, Chatterjee A, Torres G (2021). A state-space approach to understand responses  
1037 of organisms, populations and communities to multiple environmental drivers. *Comms Biol*  
1038 4:1142.

1039 Giménez L, Espinosa N, Torres G (2022). A framework to understand the role of biological  
1040 time in responses to fluctuating climate drivers. *Sci Rep* 12:10429.

1041 Gunderson A, Armstrong E, Stillman J (2016) Multiple stressors in a changing world: the  
1042 need for an improved perspective on physiological responses to the dynamic marine  
1043 environment. *Annu Rev Mar Sci* 8:357–378.

1044 Guerrero F, Blanco JM, Rodríguez V (1994) Temperature-dependent development in marine  
 1045 copepods: a comparative analysis of models. *J Plankton Res* 16: 95-103.  
 1046 Gvoždík L (2018). Just what is the thermal niche? *Oikos* 127:1701–1710.  
 1047 Hazel WN, Smock R, Johnson MD (1990). A polygenic model for the evolution and  
 1048 maintenance of conditional strategies. *Proc R Soc B* 242:81–187.  
 1049 Hobday AJ, Alexander LV, Perkins SE, Smale DA, Straub SC, Oliver ECJ Benthuisen JA,  
 1050 Burrows MT, Donat MG, Feng M, Holbrook NJ, Moore P Scannell HA, Gupta AS,  
 1051 Wernberg T . (2016). A hierarchical approach to defining marine heatwaves. *Prog Oceanogr*  
 1052 141:227–238.  
 1053 Hoffmann AA, Sorensen JG, Loeschke V (2003). Adaptation of *Drosophila* to temperature  
 1054 extremes: bringing together quantitative and molecular approaches. *J Therm Biol* 28:175.  
 1055 Jackson MC, Pawar S, Woodward, G. (2021) Temporal dynamics of multiple stressor effects:  
 1056 from individuals to ecosystems. *Trends Ecol Evol* 36:402–410.  
 1057 Jacox MG (2019). Marine heatwaves in a changing climate. *Nature* 571:485–486.  
 1058 Jørgensen LB, Malte H, Overgaard J (2019). How to assess *Drosophila* heat tolerance:  
 1059 Unifying static and dynamic tolerance assays to predict heat distribution limits. *Funct Ecol*  
 1060 33:629–642.  
 1061 Koussoroplis AM, Pincebourde S, Wacker A (2017) Understanding and predicting  
 1062 physiological performance of organisms in fluctuating and multifactorial environments. *Ecol*  
 1063 *Monogr* 87: 178–197.  
 1064 Kreyling J, Jentsch A, Beier C (2014). Beyond realism in climate change experiments:  
 1065 gradient approaches identify thresholds and tipping points. *Ecol Lett* 17:125–e1.  
 1066 Kreyling J, Schweiger AH, Bahn M, Ineson P, Migliavacca M, Morel-Journel T, Christiansen  
 1067 JR, Schtickzelle N, Larsen KS (2018). To replicate, or not to replicate – that is the question:  
 1068 how to tackle nonlinear responses in ecological experiments. *Ecol Lett* 21:629–1638.  
 1069 Kroeker KJ Bell LE, Donham EM, Hoshijima U, Lummis S, Toy J, Willis-Norton E (2020)  
 1070 Ecological change in dynamic environments: Accounting for temporal environmental  
 1071 variability in studies of ocean change biology. *Glob Change Biol.* 26: 54–67.

1072 Laubach ZM, Holekamp KE, Aris, IM, Slopen N, Perng W (2022). Applications of  
 1073 conceptual models from lifecourse epidemiology in ecology and evolutionary biology. *Biol*  
 1074 *Lett* 18:20220194.

1075 Legendre P, Legendre L (2012). *Numerical Ecology*. Elsevier.

1076 Levins R (1968) *Evolution in changing environments: some theoretical explorations*.  
 1077 *Monographs in Population Biology* 2. Princeton.

1078 Lynch HJ, Rhainds M, Calabrese JM, Cantrell, S, Cosner C, Fagan WF (2014). How climate  
 1079 extremes-not means- define a species' geographic range boundary via a demographic tipping  
 1080 point. *Ecol Monogr* 84:131–149.

1081 Maggi E, Bulleri F, Bertocci I, Benedetti-Cecchi L (2012). Competitive ability of macroalgal  
 1082 canopies overwhelms the effects of variable regimes of disturbance. *Mar Ecol Prog Ser*  
 1083 465:99–109

1084 Manenti T, Loeschcke V, Sørensen JG (2018). Constitutive up-regulation of *Turandot* genes  
 1085 rather than changes in acclimation ability is associated with the evolutionary adaptation to  
 1086 temperature fluctuations in *Drosophila simulans*. *J Insect Physiol* 104:40–47.

1087 Marshall DJ, Burgess SC, Connallon T (2016). Global change, life-history complexity and  
 1088 the potential for evolutionary rescue. *Evol Appl* 9:1189–1201.

1089 McLaren I (1995) Temperature-dependent development in marine copepods: comment on  
 1090 choices of models. *J Plankton Res* 17: 1385–1390.

1091 Minuti JJ, Byrne M, Campbell H, Hemraj DA, Russell BD (2022). Live-fast-die-young:  
 1092 Carryover effects of heatwave-exposed adult urchins on the development of the next  
 1093 generation. *Glob Change Biol* 28:5781–5792.

1094 Munch SB, Rogers TL, Symons CC, Pennekamp F (2023) Constraining nonlinear time series  
 1095 modeling with the metabolic theory of ecology. *Proc Natl Acad Sci USA* 120:e2211758120.

1096 Needham T (2021) *Visual differential geometry and forms*. Princeton University Press.

1097 Niehaus AC, Angilletta MJ, Sears MW, Franklin CE, Wilson RS (2012). Predicting the  
 1098 physiological performance of ectotherms in fluctuating thermal environments. *J Exp Biol*  
 1099 215:694–701.

1100 Pechenik J (2006). Larval experience and latent effects—metamorphosis is not a new  
 1101 beginning, *Integr Comp Biol* 46:323–333.



1102 Pörtner HO, Schulte PM, Wood CM, Schiemer F (2010). Niche dimensions in fishes: An  
 1103 Integrative View. *Physiol Biochem Zool* 83:808–826.

1104 Pratchett MS, Munday PL, Wilson SK, Graham NA, Cinner JE, Bellwood DR, Jones JP,  
 1105 Polunin NV, McClanahan TR (2008) Effects of climate -induced coral bleaching on coral  
 1106 reef fishes – ecological and economic consequences. *Oceanogr Mar Biol Annu Rev* 48: 251–  
 1107 296.

1108 Ontiveros VJ, Capitán JA, Casamayor EO, Alonso D (2021). The characteristic time of  
 1109 ecological communities. *Ecology* 102:e03247.

1110 Ponti R, Sannolo M (2022). The importance of including phenology when modelling species  
 1111 ecological niche. *Ecography* e06143.

1112 Pörtner HO (2002). Climate variations and the physiological basis of temperature dependent  
 1113 biogeography: systemic to molecular hierarchy of thermal tolerance in animals. *Comp*  
 1114 *Biochem Physiol A* 132:739–761.

1115 Quinn BK (2021). Performance of the SSI development function compared with 33 other  
 1116 functions applied to 79 arthropod species’ datasets. *J Thermal Biol* 102:103–112.

1117 Reid JM, Acker P (2022). Properties of phenotypic plasticity in discrete threshold traits.  
 1118 *Evolution* 76:190–206.

1119 Rezende EL, Castañeda LE, Santos M (2014). Tolerance landscapes in thermal ecology.  
 1120 *Funct Ecol* 28:799–809.

1121 Roman & Pierson 2022,

1122 Rombough P (2003) Modelling developmental time and temperature. *Nature* 424:268–269

1123 Romero-Mujalli D, Rochow M, Kahl S, Paraskevopoulou S, Folkertsma R, Jeltsch F, *et al.*  
 1124 (2021). Adaptive and nonadaptive plasticity in changing environments: Implications for  
 1125 sexual species with different life history strategies. *Ecol Evol* 11:6341–6357.

1126 Ruiz-Herrera A (2017). Carry-over effects: population abundance, ecological shifts, and the  
 1127 (dis-)appearance of oscillations. *Ecol Mod* 349:26–32.

1128 Russo S, Sillmann J, Fischer EM (2015). Top ten European heatwaves since 1950 and their  
 1129 occurrence in the coming decades. *Environ Res Lett* 10:124003.

1130 Sæther B-E, Engen S (2015). The concept of fitness in fluctuating environments. *Trends Ecol*  
 1131 *Evol* 30:273–281.

1132 Salachan PV, Sørensen JG (2022). Molecular mechanisms underlying plasticity in a  
 1133 thermally varying environment. *Molec Ecol* 31:3174–3191.

1134 Rezende EL, Santos M (2012). Comment on ‘Ecologically relevant measures of tolerance to  
 1135 potentially lethal temperatures’ *Exp Biol* 215:702–703.

1136 Šargač Z, Giménez L, González-Ortegón E, Harzsch S, Tremblay N, Torres G (2022)  
 1137 Quantifying the portfolio of larval responses to salinity and temperature in a coastal-marine  
 1138 invertebrate: a cross population study along the European coast. *Mar Biol* 169:81

1139 Scheiner SM (2016). Habitat choice and temporal variation alter the balance between  
 1140 adaptation by genetic differentiation, a jack-of-all-trades strategy, and phenotypic plasticity.  
 1141 *Am Nat* 187:633–646.

1142 Schweiger AH, Irl SDH, Steinbauer MJ, Dengler J, Beierkuhnlein C (2016). Optimizing  
 1143 sampling approaches along ecological gradients. *Methods Ecol Evol* 7: 463–471.

1144 Seebacher F, Beaman J, Little AG (2014). Regulation of thermal acclimation varies between  
 1145 generations of the short-lived mosquitofish that developed in different environmental  
 1146 conditions. *Funct Ecol* 28:137–148.

1147 Schindler DE, Armstrong JB, Reed TE (2015). The portfolio concept in ecology and  
 1148 evolution. *Front Ecol Environ* 13:257–263.

1149 Shi P-J, Reddy GVP, Chen L, Ge F (2016). Comparison of thermal performance equations in  
 1150 describing temperature-dependent developmental rates of insects: (II) Two Thermodynamic  
 1151 Models. *Ann Entom Soc America* 110:113–120.

1152 Smith MD (2011). An ecological perspective on extreme climatic events: a synthetic  
 1153 definition and framework to guide future research. *J Ecol* 99:656-663.

1154 Stearns S (1986). *Evolution of life histories*. Oxford Univ Press.

1155 Tang J, Ikediala JN, Wang S, Hansen JD, Cavalieri RP (2000). High-temperature-short-time  
 1156 thermal quarantine methods. *Postharvest Biol Technol* 21:129–145.

1157 Terblanche JS, Hoffmann AA, Mitchell KA, Rako L, le Roux PC, Chown SL (2011).  
 1158 Ecologically relevant measures of tolerance to potentially lethal temperatures. *J Exp Biol*  
 1159 214:3713–3725.

1160 Thompson RM, Beardall J, Beringer J, Grace M, Sardina P (2013) Means and extremes:  
 1161 building variability into community-level climate change experiments. *Ecol Lett* 16:799–806.

1162 Torres G, Giménez L (2020). Temperature modulates compensatory responses to food  
 1163 limitation at metamorphosis in a marine invertebrate. *Funct Ecol* 34:1564–1576.

1164 Torres G, Charmantier G, Wilcockson D, Harzsch S, Giménez L (2021) Physiological basis  
 1165 of interactive responses to temperature and salinity in coastal marine invertebrate:  
 1166 Implications for responses to warming. *Ecol Evol* 11:7042–7056.

1167 Torres G, Giménez L, Pettersen AK, Bue M, Burrows MT, Jenkins SR (2016) Persistent and  
 1168 context-dependent effects of the larval feeding environment on post-metamorphic  
 1169 performance through the adult stage. *Mar Ecol Prog Ser* 545:147–160.

1170 Turner MG, Romme WH, Gardner RH, Oneill RV, Kratz TK (1993) A revised concept of  
 1171 landscape equilibrium: disturbance and stability on scaled landscapes. *Landsc Ecol* 8:213–  
 1172 227.

1173 Uller T, Nakagawa S, English S (2013) Weak evidence for anticipatory parental effects in  
 1174 plants and animals. *J Evol Biol*, 26, 2161–2170.

1175 Urban HJ (1994) Upper temperature tolerance of ten bivalve species off Peru and Chile  
 1176 related to El Nino. *Mar Ecol Prog Ser* 107: 139–145.

1177 Vasseur DA, Yodzis P (2004) The color of environmental noise. *Ecology* 85:1146–1152.

1178 Vinebrooke D, Cottingham RL, Norberg K, Scheffer M, Dodson JI, Maberly SC, Sommer U  
 1179 (2004). Impacts of multiple stressors on biodiversity and ecosystem functioning: the role of  
 1180 species co-tolerance. *Oikos* 104:451-457.

1181  
 1182